Australian Government
Department of Defence
Defence Science and
Technology Organisation

# Calculations of the Sound Scattering of Hyperbolic Frequency Modulated Chirped Pulses from Fluid-filled Spherical Shell Sonar Targets

*Mark Readhead*

**Maritime Operations Division**
**Defence Science and Technology Organisation**

DSTO-RR-0351

## ABSTRACT

The theory of the sound pressure scattered from a fluid-filled spherical shell immersed in a second fluid is developed for the case of ensonification with hyperbolic frequency modulated chirped pulses. Hyperbolic frequency modulation is also known as 'linear period modulation' and 'logarithmic phase modulation'. The theory is used to calculate the target strength of a stainless steel shell filled with a mixture of Freon-113™ and ethanol, and immersed in sea water. The sensitivity of the target strength to pulse centre frequency, pulse bandwidth, pulse length and fluid temperature is examined and significant sensitivity is found in some cases, especially for temperature. The signal reflected by the target is shown as a function of time, and the results of correlating the return with a replica of the transmitted signal are also shown. Comparison is made with a solid stainless steel sphere and air-filled spherical shells, and similar parameter sensitivity is found, with the exception that their target strengths are insensitive to temperature.

## RELEASE LIMITATION

*Approved for public release*

*Published by*

*Maritime Operations Division*
*DSTO Defence Science and Technology Organisation*
*PO Box 1500*
*Edinburgh South Australia 5111 Australia*

*Telephone: (08) 8259 5555*
*Fax: (08) 8259 6567*


*AR-014-725*
*February 2010*

**APPROVED FOR PUBLIC RELEASE**

# Calculations of the Sound Scattering of Hyperbolic Frequency Modulated Chirped Pulses from Fluid-filled Spherical Shell Sonar Targets

## Executive Summary

Target detection range is an important parameter in sonar performance assessment. Ideally, assessments should be made using targets with well-known acoustic scattering efficiency or "target strength". Fluid-filled spherical shells have been used as sonar targets because they scatter sound independently of look direction or "aspect", and have target strengths that are large in comparison to their size. Readhead (1995) studied the characteristics of fluid-filled shells under ensonification by continuous tones, tone bursts and linear frequency modulated chirped pulse waveforms. The hyperbolic frequency modulated chirped pulse waveform is also widely used in wideband active sonar design as a way of minimising the degradation of matched filter processing when the source and target are in relative motion. Sonars using these waveforms are now being assessed by the DSTO and the Royal Australian Navy for various applications. This report extends the work of Readhead (*op. cit.*) to consider the use of fluid-filled spherical shells in assessing the performance of such sonars.

Readhead (*op. cit.*) considered the acoustic scattering efficiency of fluid-filled spherical shells as a function of their physical parameters, including shell material, diameter, wall thickness and filling fluid. This report fixes those parameters to stainless steel shells in use by the Commonwealth of Australia and its contractors. The shells have 20 cm diameter with a wall thickness of 0.9 mm, and are filled with a mixture of 68% Freon-113™ and 32% ethanol by volume. The shells are deployed at shallow depths in sea water of 35‰ salinity, with temperatures varying between 5 and 35°C. The variation of the target strength is examined as a function of frequency up to 450 kHz, bandwidth between 1 and 50 kHz, pulse length between 50 μs and 5 ms, and temperature between 5 and 35°C.

For a fixed frequency, the target strength is insensitive to bandwidth and pulse length. However the target strength varies with small changes in frequency. This variation is higher for longer duration pulses, but is reduced as the bandwidth increases.

There is some sensitivity of the target strength to water temperature. At frequencies *above* 200 kHz, the variation of target strength with frequency at temperatures above and below 20°C is quite different: below 20°C the target strength generally increases with frequency; whereas above 20°C it decreases with frequency. Above 300 kHz the target strength generally decreases with increasing temperature, with a decline of more than 10 dB as the temperature increases from 5 to 35°C.

*Below* 200 kHz, the target strength does not vary by more than a few decibels over the temperature range of 5 to 35°C, with the variation remaining less than 2 dB for temperatures between 15 and 25°C. The maximum target strength is attained at a

temperature of about 20°C. At 100 kHz the target strength variation with temperature is quite smooth and it varies by no more than 1 dB between 15 and 25°C.

The target strength for small bandwidth, long duration signals is strongly dependent on temperature, as was the case for continuous tone signals discussed in Readhead (*op. cit.*). For example, at 100 kHz a 5 ms pulse with a 1 kHz bandwidth results in a target strength variation of up to 3 dB over a 2°C temperature change.

Solid and air-filled spheres are sometimes considered as alternate aspect-independent targets, and their response to hyperbolic frequency modulated chirped pulses is also examined. Targets considered are a solid 20 cm diameter stainless steel sphere, and air-filled stainless steel shells of the same exterior diameter, with wall thicknesses of 0.5, 2, 5 and 10 mm. Both types of target have considerably lower target strengths than a fluid-filled sphere of the same diameter – in the case of the air-filled spheres, by more than 15 dB. Although these alternate targets show almost no sensitivity of the target strength to water temperature, they show more sensitivity than fluid-filled spheres to small changes in frequency when chirped pulses are used. If the bandwidth is small, target strength changes of 5 – 12 dB can occur when the frequency changes by a few kilohertz. This may be a problem for sonars which switch between closely spaced frequency bins of narrow bandwidth in order to spatially resolve target returns.

Examining the returned signal in the time domain, for all three target types a short pulse length gives the clearest returns. As the duration of the impinging signal increases there is overlap of signals reflected from different parts of the target. Changing the bandwidth of the signal does not help to elucidate details of the target.

When matched filtering is employed for target detection, it is common for a replica of the outgoing waveform to be cross-correlated with the reflected signal. In this case, decreasing the pulse length or increasing the bandwidth sharpens the range resolution for all targets. Increasing the pulses length makes little difference to the target strength. Increasing the bandwidth makes almost no difference to the target strength of the fluid-filled sphere, but does increase the target strength of the solid and air-filled spheres by 1 – 2 dB.

In comparing fluid-filled and air-filled spheres as sonar targets, not only is the target strength of the former substantially higher than the latter, but the fluid-filled sphere is also slightly less prone to target strength variability.

# Author

**Mark Readhead**
Maritime Operations Division

*Mark Readhead obtained a BSc (Hons) in Physics from the University of Western Australia in 1979, and a PhD in Physics from the Australian National University in 1984. After lecturing in Physics and holding the position of Postdoctoral Research Associate at the University of Washington, he joined DSTO in 1989. In 1995 he won the inaugural RAN Science Scholarship and studied acoustic imaging using underwater ambient noise at the Scripps Institution of Oceanography. He works in the Maritime Operations Division and current research interests include the performance of fluid-filled spherical shells, target strengths of sea mines, absorption of sound by sea water, thermal noise, the distribution of underwater noise sources, acoustic imaging with ambient noise, and high frequency sonars.*

# Contents

# 1. Introduction

Over the past 20 years DSTO has supplied fluid-filled spheres to the Royal Australian Navy and its contractors, who have used them to assess the target detection performance of high-frequency active sonars. Readhead (1995) presented the theory describing the performance of the spheres, emphasising their target strength and its dependence on a selection of physical parameters. More recently, similar spheres have been used in trials of sonars that emit hyperbolic frequency modulated chirped pulses. These trials have been conducted in waters with a range of different temperatures. As noted in Readhead (*op. cit.*), the target strength of these types of spheres is liable to change with ambient water temperature. The degree of variation could potentially distort the results of sonar detection range trials.

The hyperbolic frequency modulated chirp waveform, also known as a linear period modulated or logarithmic phase modulated chirp, is widely used in wideband active sonar design as a way of minimising the degradation of matched filter processing caused by Doppler shifting of the return signal when the source and target are in relative motion. The theory of Readhead (*op. cit.*) is extended to cover this waveform, and results are presented in a variety of ways. The target strength is shown for chirps of 50, 500 and 5000 μs duration, bandwidths between 1 and 50 kHz, and water temperatures between 5 and 35°C. The signal reflected by the target is shown as a function of time, and the results of correlating the return with a replica of the transmitted signal are also shown. Comparison is also made with a solid sphere and air-filled spherical shells.

# 2. Theory

## 2.1 Geometry

Consider a fluid medium of infinite extent whose density is $\rho_1$ and which supports longitudinal sound waves of speed $c_1$. A fluid-filled spherical shell is located at the origin of a spherical coordinate system, as shown in Figure 1. The inner and outer radii of the shell are $a$ and $b$, respectively. The shell has a density $\rho_2$ and Poisson's ratio $\sigma$, and supports longitudinal and transverse waves of velocity $c_{L,2}$ and $c_{T,2}$, respectively. The interior fluid has a density of $\rho_3$ and longitudinal sound speed of $c_3$.

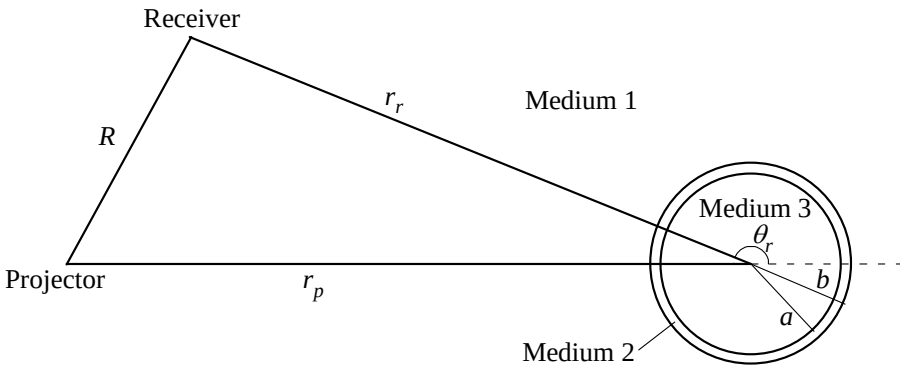


*Figure 1: Geometry for projector, receiver and fluid-filled sphere.*

## 2.2 Continuous waves

Readhead (*op. cit.*) considered a point source of sound located at $r = r_p$ and $\theta = 0$ with respect to the origin. When emitting continuous sinusoidal sound waves, the incident pressure a distance *R* away in the external fluid was

$$P_i = P_0 \frac{e^{i(2\pi ft - k_{L,1}R)}}{R} \tag{1}$$

where $P_0$ was the amplitude of the pressure wave 1 m from the source, *f* was the frequency of the wave and $k_{L,1}$ was the wavenumber in the fluid, related to the frequency by

$$k_{L,1} = \frac{2\pi f}{c_1}. \tag{2}$$

The time component of the waves was ignored, and the displacement component of the incident pressure was

$$p_i = P_0 \frac{e^{-ik_{L,1}R}}{R}. \tag{3}$$

It was shown that the scattered pressure at the listening point $r = r_r$ and $\theta = \theta_r$ was

$$p_s = P_0 k_{L,1} \sum_{l=0}^{\infty} (-1)^l (2l+1) C_l h_l^* \left(k_{L,1} r_p\right) h_l^* \left(k_{L,1} r_r\right) P_l \left(\cos\theta_r\right) \qquad \text{for } 0 < r_r < r_p \tag{4}$$

where $h_l$ and $P_l$ were spherical Hankel and Legendre functions of order *l*. The $C_l$ were coefficients dependent on spherical Bessel, Neumann and Hankel functions, their first and second derivatives, and parameters *f*, $\rho_1$, $\rho_2$, $\rho_3$, $\sigma$, *a*, *b*, $c_1$, $c_{L,2}$, $c_{T,2}$ and $c_3$.

## 2.3 Hyperbolic frequency modulated chirped pulses

In the above equations the point source was considered as producing sinusoidal waves. Readhead (*op. cit.*) also considered the scattered pressure from tone bursts and linear frequency modulated chirped pulses. The scattered pressure from hyperbolic frequency modulated chirped pulses will now be considered.

The general equation for the pressure of a frequency modulated signal of amplitude *P* is

$$p(t) = P \exp\left[2\pi i \int^t f(t')\,dt'\right] \tag{5}$$

where $f(t)$ is the instantaneous frequency of the signal at time *t*. For a hyperbolic frequency modulated signal in which the frequency increases with time, Williams and Battestin (1976) give the instantaneous frequency as

$$f(t) = \frac{2 f_0 f_1}{f_0 + f_1 - \dfrac{2(f_1 - f_0)t}{\Delta t}} \qquad \text{for} \quad \frac{-\Delta t}{2} \le t \le \frac{\Delta t}{2} \tag{6}$$

where $f_0$ is the start frequency, $f_1$ is the stop frequency and $\Delta t$ is the pulse length.

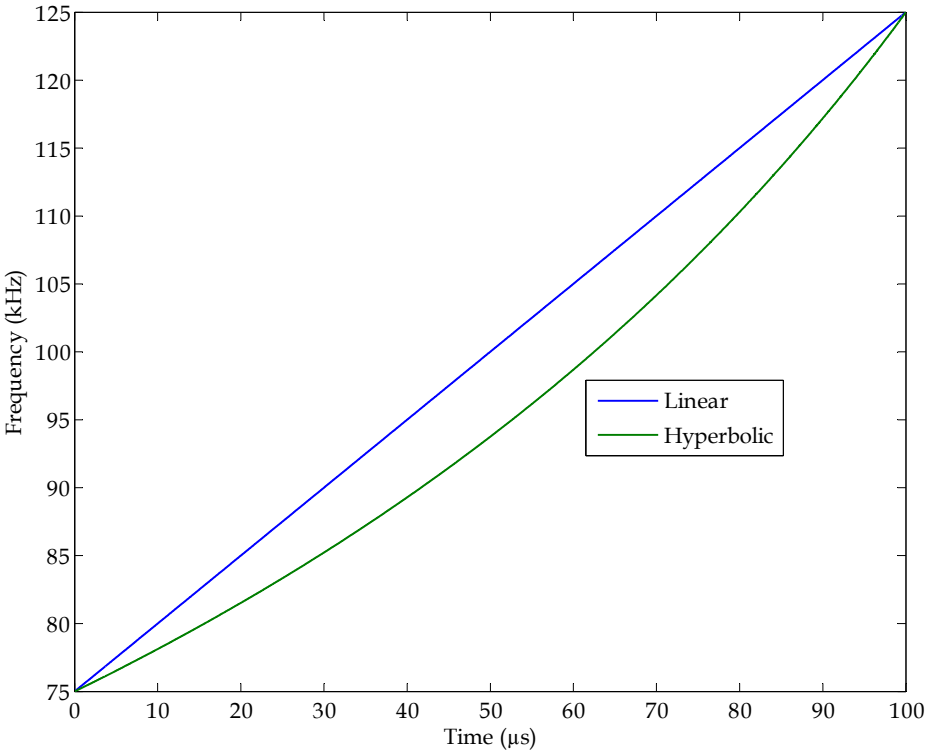


*Figure 2: The instantaneous frequency of linear and hyperbolic frequency modulated chirped pulses of 100 µs duration and 50 kHz bandwidth centred on 100 kHz.*

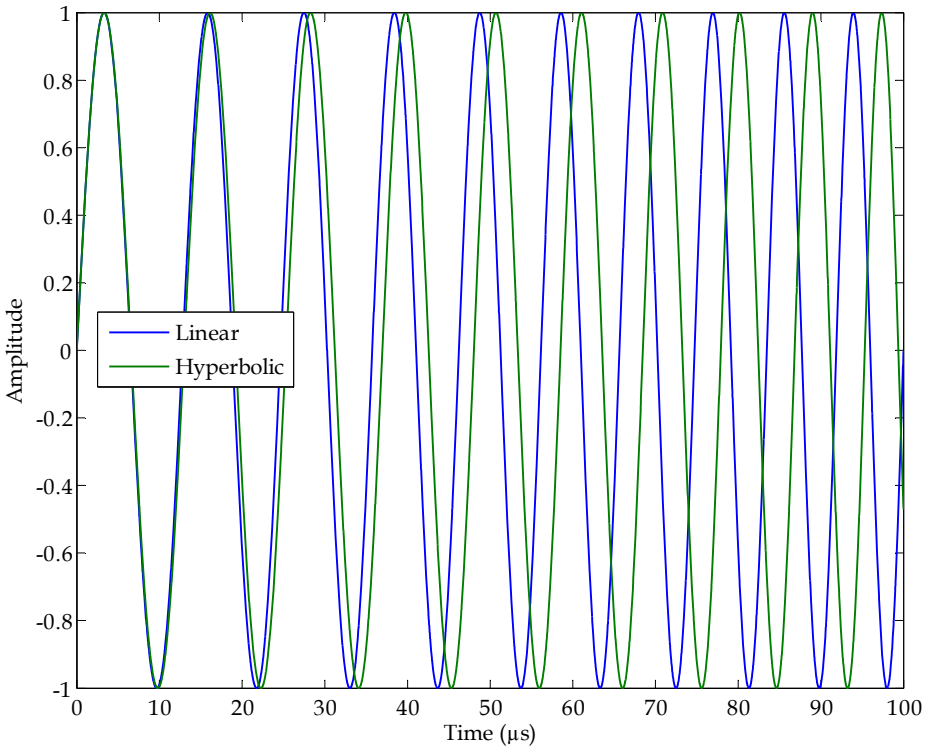


*Figure 3: The amplitude of linear and hyperbolic frequency modulated chirped pulses of 100 µs duration and 50 kHz bandwidth centred on 100 kHz.*

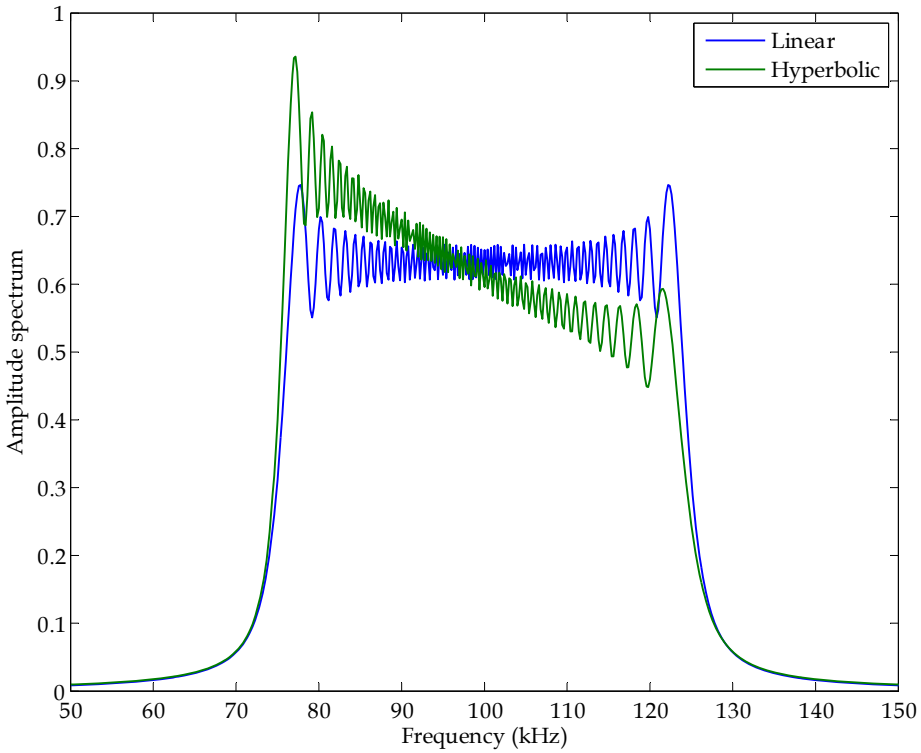


*Figure 4: The amplitude spectra of linear and hyperbolic frequency modulated chirped pulses of 5 ms duration and 50 kHz bandwidth centred on 100 kHz.*

Figure 2 plots the instantaneous frequency of a hyperbolic frequency modulated chirped pulse as a function of time, and compares it to the linear frequency modulated chirped pulse. In both cases the sweep frequency increases with time. Figure 3 compares their amplitudes as a function of time, and Figure 4 compares their spectra, calculated from the integrands of Equation 53 in Readhead (*op. cit.*) and Equation 11. An exact formula for the spectrum of the hyperbolic frequency modulated chirped pulse is also given in Kroszczyński (1969). It can be seen that whereas the linear frequency modulated chirped pulse has a spectrum which is symmetrical over the frequency band, the hyperbolic frequency modulated chirped pulse has an asymmetrical spectrum, although the asymmetry is less evident when the bandwidth is a smaller fraction of the centre frequency than shown in this figure.

Performing the integration in Equation 5 and substituting into Equation 1, the pressure incident on the shell becomes

$$P_i(t) = \frac{P_0}{R}\exp\left(-ik_{L,1}^c R\right)\exp\left\{-i2\pi\frac{f_0 f_1}{f_1 - f_0}\Delta t \ln\left[f_0 + f_1 - \frac{2}{\Delta t}\left(f_1 - f_0\right)t\right]\right\}\mathrm{rect}\left[\frac{1}{\Delta t}\left(t - \frac{R}{c_1}\right)\right] \qquad (7)$$

where

$$k_{L,1}^c = \frac{2\pi f_c}{c_1} \qquad (8)$$

$$f_c = \frac{2 f_0 f_1}{f_0 + f_1} \qquad (9)$$

and

$$\mathrm{rect}(t)=\begin{cases}1 & \text{for} \quad -1/2 \le t \le 1/2 \\ 0 & \text{elsewhere}\end{cases}. \tag{10}$$

The incident signal frequency components are obtained by taking the Fourier transform of Equation 7, or

$$P_i(f)=\frac{P_0}{R}e^{-ik_{L,1}R}\int_{-\Delta t/2}^{\Delta t/2} e^{-i2\pi\frac{f_0 f_1}{f_1-f_0}\Delta t \ln\left[f_0+f_1-\frac{2}{\Delta t}(f_1-f_0)t\right]}e^{-i2\pi ft}dt. \tag{11}$$

The scattered frequency components are

$$P_s(f)=p_s(f)\int_{-\Delta t/2}^{\Delta t/2} e^{-i2\pi\frac{f_0 f_1}{f_1-f_0}\Delta t \ln\left[f_0+f_1-\frac{2}{\Delta t}(f_1-f_0)t\right]}e^{-i2\pi ft}dt \tag{12}$$

where $p_s$ is given by Equation 4. The scattered pressure may then be obtained by the inverse Fourier transform. As a function of time

$$P_s(t)=\int_{-\infty}^{\infty} p_s(f)\left\{\int_{-\Delta t/2}^{\Delta t/2} e^{-i2\pi\frac{f_0 f_1}{f_1-f_0}\Delta t \ln\left[f_0+f_1-\frac{2}{\Delta t}(f_1-f_0)t\right]}e^{-i2\pi ft}dt\right\}e^{i2\pi ft}df. \tag{13}$$

## 2.4 Target strength

The parameters of the sonar equations (Horton, 1959), of which the target strength is one parameter, are normally expressed as intensities and are applicable to pulses of constant intensity under steady state conditions (Urick, 1962). The target strength is defined as 10 times the logarithm to the base 10 of the ratio of the intensity of the sound returned by the target, at a distance of 1 m from its acoustic centre in some direction, to the incident intensity from a distant source (Urick, 1983). Note that it is not a function of the return signal only, but is a ratio of intensities, and to make numerical sense both the incident and returned intensities must be calculated or measured in the same manner.

In measuring a target strength, it is not practical to measure the scattered sound 1 m from the target's acoustic centre. In what Urick (1983) refers to as the "conventional method" of target strength measurements, the measurements are made at a long range and then reduced to what they would be at 1 m. The long range is taken to be in the far field, where the target appears to reradiate as a point source of sound. The start of the far field is defined (Urick, 1983; Medwin and Clay, 1998) as

$$r=\frac{L^2}{\lambda} \tag{14}$$

where $L$ is the maximum dimension of the target as seen by the receiver and $\lambda$ is the wavelength of sound. Bobber (1988) uses the same equation, but notes that it is "very conservative".

Urick (1962) generalised the sonar equations to cover transients, and in this redefinition the quantities are based on the total acoustic energy associated with a pulse, rather than on the mean rate of energy flow. The target strength is still the long-pulse steady state quantity, and as pointed out by Chu and Stanton (1998), it incorporates the total scattered wave from the target, without distinguishing between various partial waves which might make up that signal. Urick's (1962) generalised equations have been explicitly applied to wideband transmissions (Nelson, 1976).

Combining the conventional method with the generalised sonar equations, the backscattered target strength for a pulsed incident signal of constant amplitude is

$$TS = 10\log\left(\frac{r_p^2 r_r^2}{P_0^2 \Delta t}\int_t^\infty \left|P_s(t')\right|_{r=r_r}\Big|^2 dt'\right) \tag{15}$$

when $\theta = 180°$ and $r_p$ and $r_r$ are in the far field. The integration starts with the first return, which arrives at

$$t = \frac{r_p + r_r - 2b}{c_1} - \frac{\Delta t}{2} \tag{16}$$

In the results reported below, both $r_r$ and $r_p$ are set to 1000 m to ensure far field conditions, and the physical data used for $\rho_1$, $\rho_2$, $\rho_3$, $\sigma$, $c_1$, $c_{L,2}$, $c_{T,2}$ and $c_3$ are as in Readhead (*op. cit.*). This equation for target strength differs somewhat from Readhead (*op. cit.*), who calculated the target strength of the most intense partial wave, a quantity termed the "effective target strength" by Kaduchak and Loeffler (1998).

# 3. Results

## 3.1 Frequency, band width and pulse length variations

In the results which follow, three types of targets are considered, as detailed in Table 1. The main target considered is a spherical shell of stainless steel with a diameter of 20 cm and 0.9 mm wall thickness. This shell is filled with a mixture of 68% Freon-113™ and 32% ethanol by volume. This target will be referred to as the 'fluid-filled sphere'. Comparison is made to two other types of target. One is a solid stainless steel sphere of 20 cm diameter. This will be referred to as the 'solid sphere'. As air-filled shells are often used as aspect-independent targets in sonar trials, this will be the third type of target used for comparison. In this case, a spherical shell of stainless steel with a diameter of 20 cm is considered. Due to the characteristics of the backscattering performance of this type of target, four wall thicknesses will be considered, viz. 0.5, 2, 5 and 10 mm. These targets will be referred to as the '0.5 mm air-filled sphere', '2 mm air-filled sphere', etc. In all cases, the targets are assumed to be situated in shallow depths in sea water of 35‰ salinity. The projector and receiver are collocated 1000 m from the target; that is, only backscattered cases will be considered.

*Table 1: Physical properties of the stainless steel spheres.*

| Interior | Diameter (cm) | Wall thickness (mm) | Name |
|---|---|---|---|
| 68% Freon-113™ + 32% ethanol | 20 | 0.9 | Fluid-filled sphere |
| Solid | 20 | 100 | Solid sphere |
| Air | 20 | 0.5 | 0.5 mm air-filled sphere |
| Air | 20 | 2 | 2 mm air-filled sphere |
| Air | 20 | 5 | 5 mm air-filled sphere |
| Air | 20 | 10 | 10 mm air-filled sphere |

Figure 5 overlays six sets of calculated target strength values for a fluid-filled sphere deployed in sea water with an ambient temperature of 20°C. The target strength was calculated for continuous ensonification with a pure tone in 100 Hz steps from 100 Hz to 500 kHz. The target strength is also shown for 50, 500 and 5000 µs hyperbolic frequency modulated chirps of 1 and 10 kHz bandwidth centred on frequencies taken in 1 kHz steps to 450 kHz.

As noted in Readhead (*op. cit.*) the target strength for continuous tones varies greatly with small changes in frequency, is low for frequencies such that $k_{L,1}a \lesssim 4$, and takes on an oscillatory nature at high frequencies. The target strength varies much less for pulses of short duration or wide bandwidth, but oscillatory characteristics are evident at the highest frequencies in the range, except for the shortest duration chirped pulse.

Note that for long duration chirped pulses of relatively narrow bandwidth, there is significant variation of target strength with small changes of frequency. This may be a problem when the objective is to assess the target detection performance of sonars which switch between closely spaced frequency bins of narrow bandwidth in order to spatially resolve target returns.

For comparison, Figure 6 shows the target strength values for tone burst signals of 50, 500 and 5000 µs duration, overlaid on the continuous tone data. Again the longest duration tone burst produces the most variable target strength values.

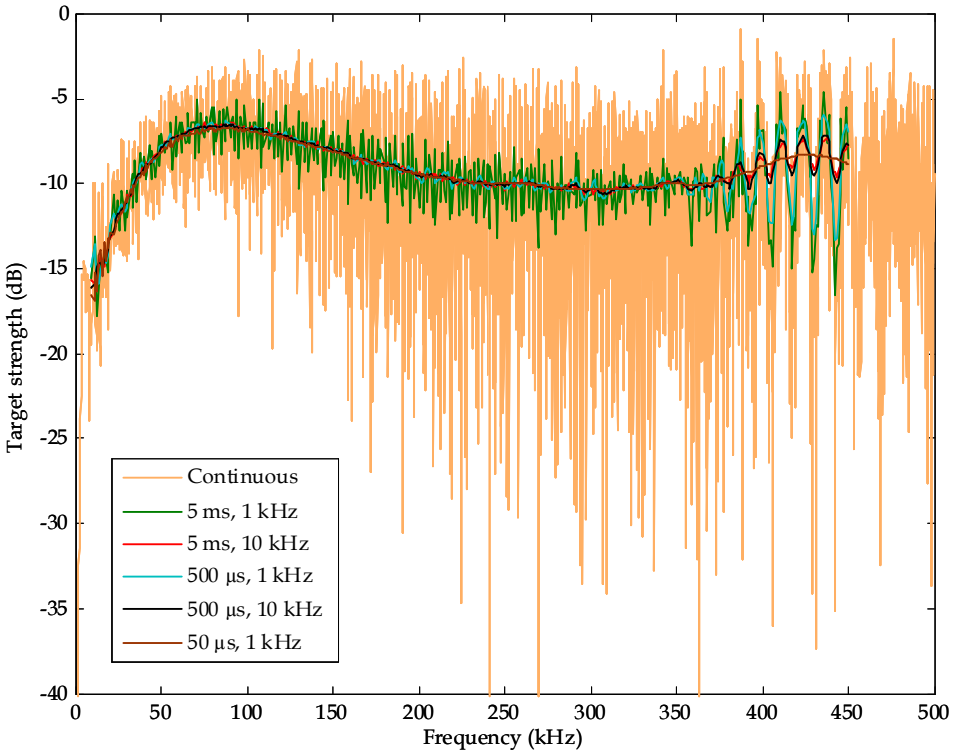


*Figure 5: Target strength of a fluid-filled sphere for continuous tones and for 1 and 10 kHz bandwidth hyperbolic frequency modulated chirps of 50 µs, 500 µs and 5 ms duration.*

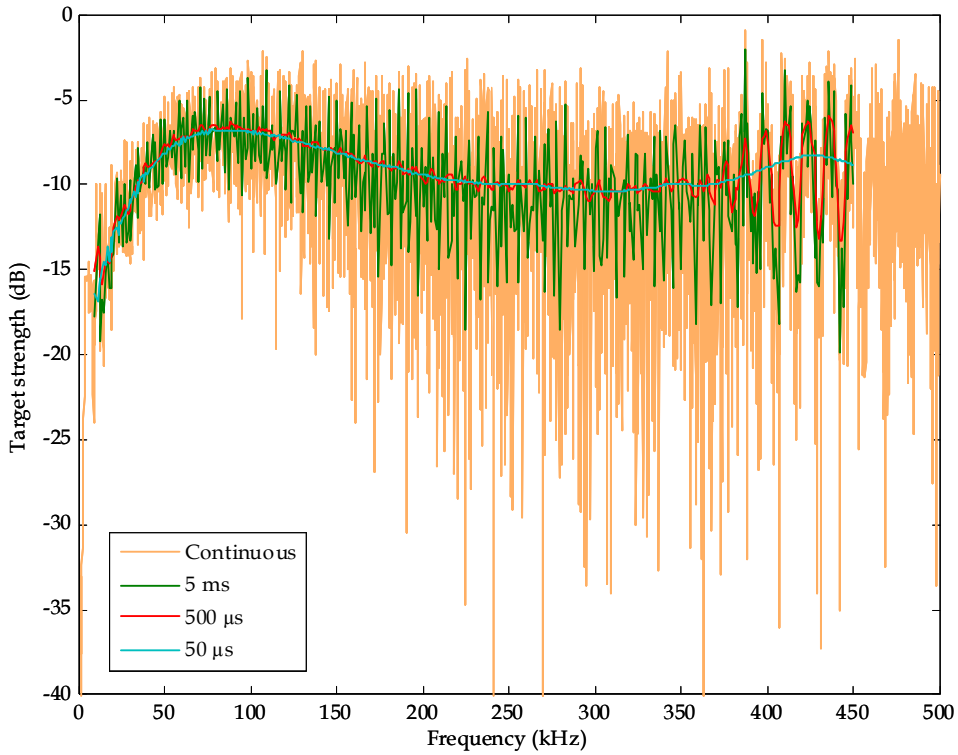


*Figure 6: Target strength of a fluid-filled sphere for continuous tones and for 50 µs, 500 µs and 5 ms tone bursts.*

In order to understand why the target strength varies with pulse length, pulse type and bandwidth, it is necessary to consider the spectrum of frequencies impinging upon the target. Figures 7 to 9 show spectra for pulse lengths of 50, 500 and 5000 µs, respectively, for tone bursts, and linear and hyperbolic frequency modulated chirped pulses of 10 kHz bandwidth. In each case, the amplitude of the signal is constant at 1 (arbitrary units) and the centre frequency is 250 kHz. The spectra for the tone bursts, and linear and hyperbolic frequency modulated chirped pulses were calculated from the sinc function in Equation 48 and the integrand of Equation 53 in Readhead (*op. cit.*), and the integrand of Equation 11, respectively. Unlike the spectra shown in Figure 4, for which the bandwidth was 50 kHz, there is almost no difference between the spectra for linear and hyperbolic frequency modulated chirped pulses for a bandwidth of 10 kHz. Also, for a pulse length of 50 µs, even the tone burst has a similar spectrum. At this pulse length, all pulse types have considerable energy in the side lobes many tens of kilohertz away from the centre frequency. The target strength will be an integration of backscattered returns over a broad range of frequencies, and will vary smoothly with changes in the centre frequency. As the pulses length increases, the energy in the side lobes decreases and that in the main lobe increases, with the effect being more pronounced for the tone burst. The integration is now over a narrower band of frequencies and so the target strength tends to follow the variations evident for continuous tones.

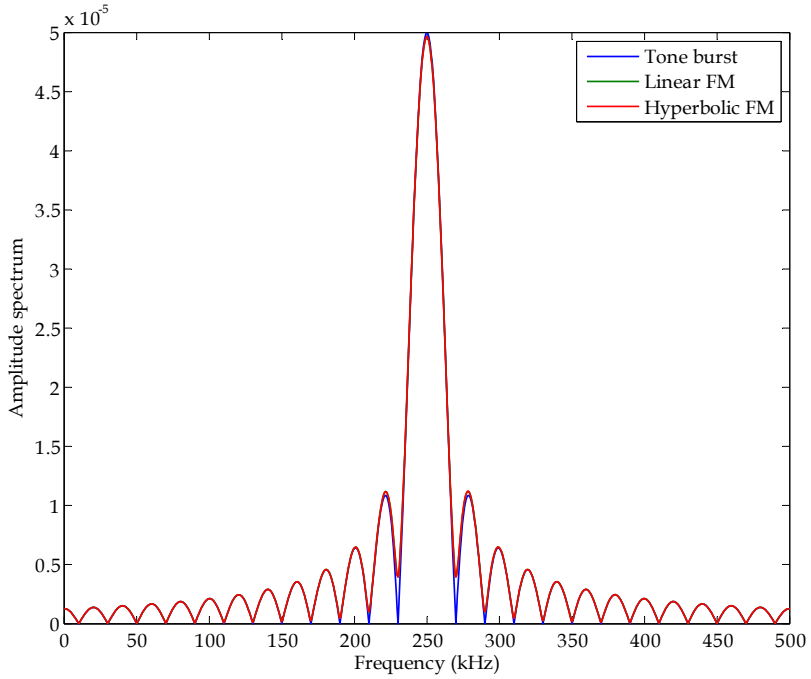


*Figure 7: The amplitude spectra of a tone burst, and linear and hyperbolic frequency modulated chirped pulses of 10 kHz bandwidth. The pulses are centred on 250 kHz and are of 50 µs duration. The curves for the linear and hyperbolic frequency modulated chirped pulses overlie each other.*

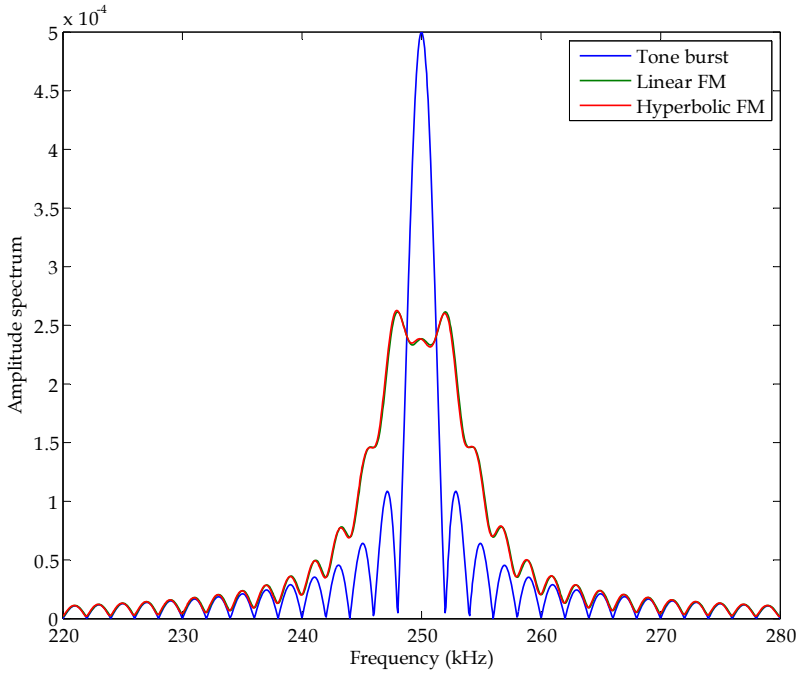


*Figure 8: The amplitude spectra of a tone burst, and linear and hyperbolic frequency modulated chirped pulses of 10 kHz bandwidth. The pulses are centred on 250 kHz and are of 500 µs duration. The curves for the linear and hyperbolic frequency modulated chirped pulses almost overlie each other.*

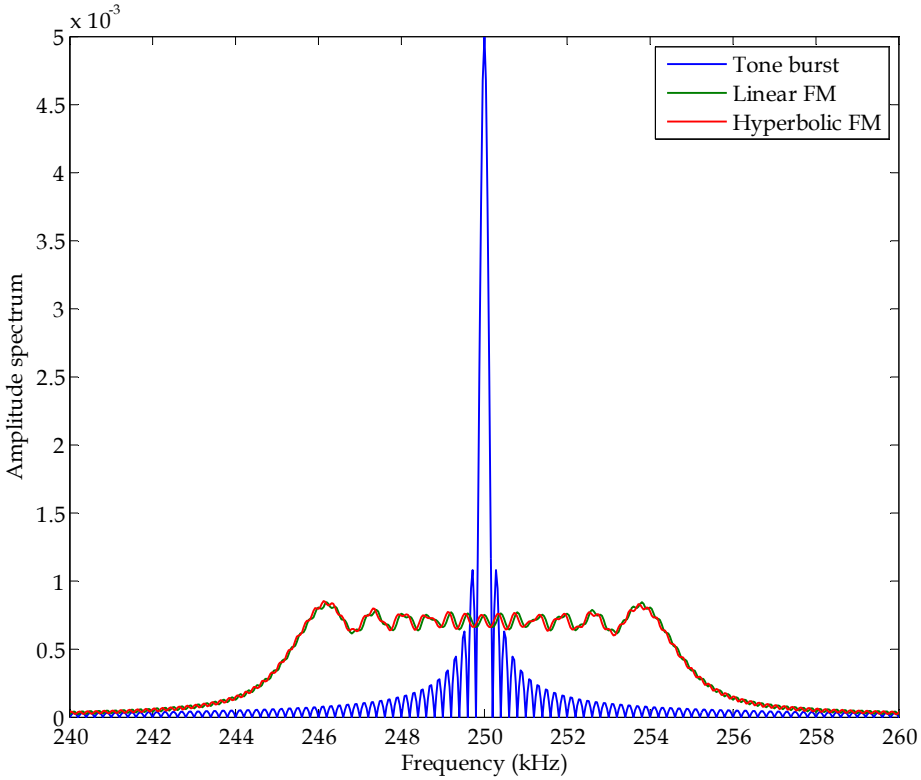


*Figure 9: The amplitude spectra of a tone burst, and linear and hyperbolic frequency modulated chirped pulses of 10 kHz bandwidth. The pulses are centred on 250 kHz and are of 5 ms duration.*

Figure 10 compares the "normal" target strength of the complete return signal calculated using Equation 15 and the "effective" target strength of the most intense partial wave as calculated from Equation 59 in Readhead (*op. cit*). The calculations have been performed for the same hyperbolic frequency modulated chirps shown in Figure 5. In all cases the "effective" target strength is less, with the difference being a function of frequency and pulse length. The most extreme difference occurs around 300 kHz and is approximately 4 dB for 50 μs and 500 μs pulses, and 0.9 dB for 5 ms pulses. At 100 kHz the greatest difference is approximately 0.5 dB. It is to be expected that the "effective" target strength will be less as the integration of the return signal is over a shorter period of time than for the "normal" target strength, whereas the integration of the incident signal is the same for both the "normal" and "effective" target strengths. Examination of the return signals in the time domain, given in section 3.2, also explains why the difference is a function of pulse length. For the shorter pulses, the partial waves are clearly separated, so an integration over the most intense partial wave omits the energy contained in the other discrete partial waves. For the 5 ms pulse most of the partial waves overlap, so the integration captures most of the energy.

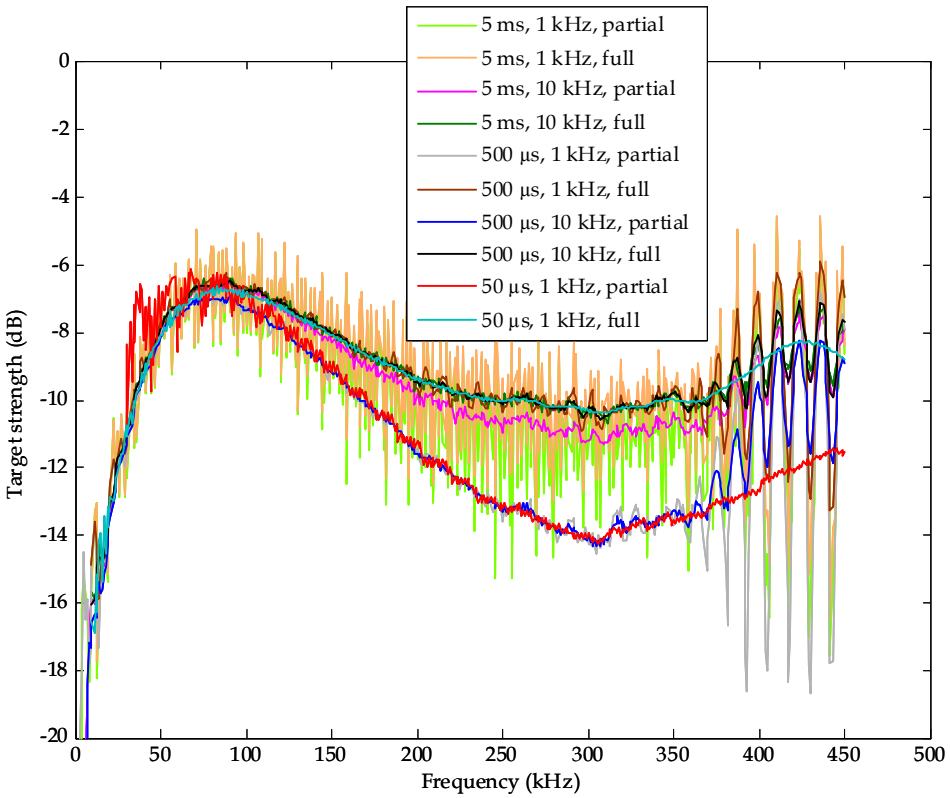


*Figure 10: "Normal" and "effective" target strength of a fluid-filled sphere for 1 and 10 kHz bandwidth hyperbolic frequency modulated chirps of 50 µs, 500 µs and 5 ms duration. The normal target strength is calculated from the full return; whereas the effective target strength is calculated from the most intense partial wave.*

In an experimental measurement of the target strength the value obtained will lie somewhere between the "normal" and "effective" target strength, as it will be difficult to distinguish between partial waves of low intensity, and reverberation and/or electronic noise in the recording system. Hence it will be necessary to end the integration of the return signal prematurely to avoid contamination by these other sources.

For the calculations reported in Figure 5, the bandwidth of the chirped pulses was held constant as the centre frequency varied. Returning to "normal" target strengths, Figure 11 presents results when the bandwidth is a constant percentage of the centre frequency, in this case 5 and 30%. With the percentages chosen the target strength varies quite smoothly with changes in centre frequency, however for the wider bandwidth the oscillations above 350 kHz no longer match those for continuous tones. This asynchronous behaviour is examined in more detail in Figure 12, which plots the target strength when the bandwidth varies between 1 and 30% of the centre frequency. As might be expected, the narrow bandwidths are associated with more variability in target strength with small changes in centre frequency, and the oscillations above 350 kHz closely follow the continuous tone case. As the bandwidth is increased the target strength becomes a smoother function of centre frequency, but the frequency of the oscillations diverge as a greater spectrum of frequencies impinge upon the target.

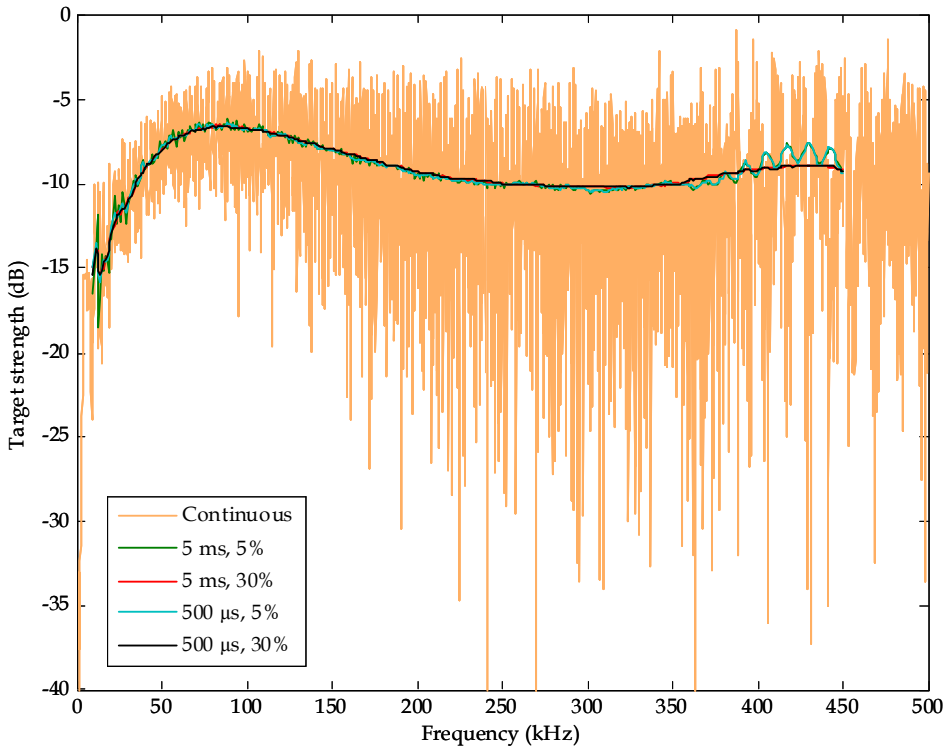


*Figure 11: Target strength of a fluid-filled sphere for continuous tones and for hyperbolic frequency modulated chirps with bandwidths of 5 and 30% of the centre frequency and of 500 µs and 5 ms duration.*

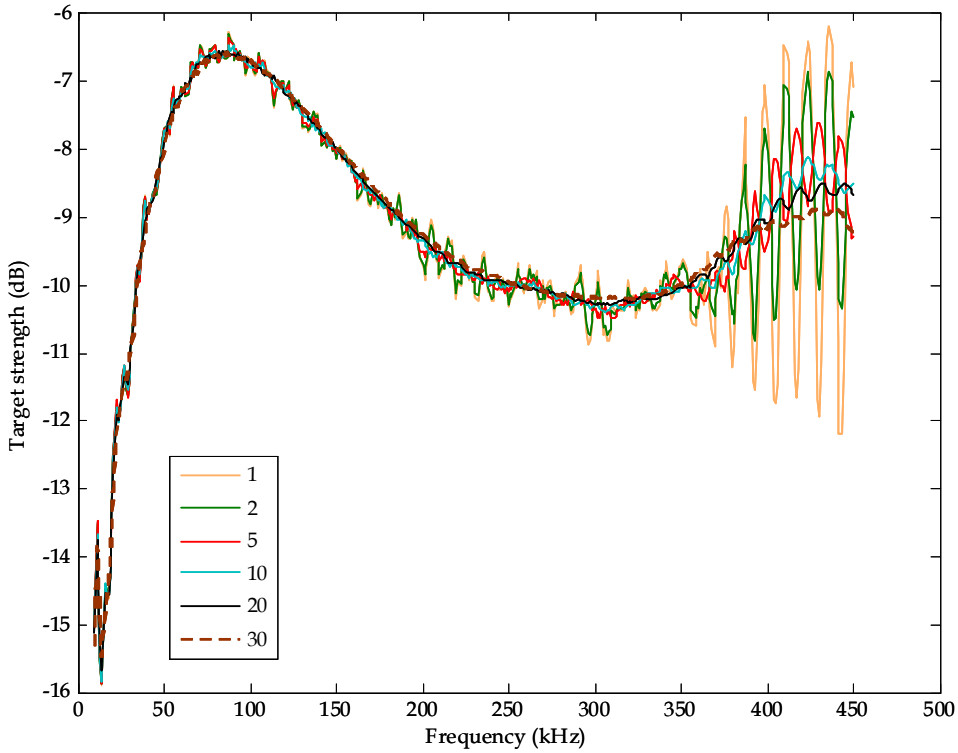


*Figure 12: Target strength of a fluid-filled sphere for 500 µs long hyperbolic frequency modulated chirps with bandwidths of 1, 2 5, 10, 20 and 30% of the centre frequency.*

A comparison of the target strength of a fluid-filled sphere is now made with the target strength of two other types of spherical target: a solid sphere and air-filled spheres. The target strength of a solid sphere is shown in Figure 13, both for continuous tones and hyperbolic frequency modulated chirps. Overall, the target strengths are lower than for a fluid-filled sphere at almost all frequencies. The change of target strength with frequency is quite periodic, the small-scale periodicity being noted by Hickling (1962). His analysis did not extend to high enough frequencies to also observe the larger-scale periodicity. It is to be noted that the target strength of the fluid-filled sphere for chirped waveforms shows considerably less oscillatory behaviour.

Air-filled spheres are commonly used as targets in sonar trials. The target strength of an ideal rigid sphere, given by Urick (1983) as

$$TS = 10\log\left(\frac{b^2}{4}\right), \tag{17}$$

is commonly assumed for air-filled spheres. However, as Hickling (1964) showed for evacuated and water-filled shells with wall thicknesses greater than $1/20\,\text{th}$ of the outer radius, the echo returned by a tone burst varies in time, and is a function of the frequency and wall thickness. In practice, a variety of wall thicknesses is used in sonar trials. For example, Kessel and Hollett (2008) used a steel sphere of 1 m diameter and 3 cm wall thickness; Trevorrow (2005) used an air-filled steel sphere of 0.914 m diameter and 6.4 mm wall thickness. Thinner walls can also be used, although they can be subject to damage, either during deployment or from the external water pressure. Standards Australia (1997) give formulae for calculating the minimum wall thickness of a spherical shell subject to external pressure.

Figures 14 to 17 show the target strength of air-filled stainless steel spheres of 20 cm diameter, for wall thicknesses of 0.5, 2, 5 and 10 mm, respectively. Again, at most frequencies, the target strengths are lower than for the fluid-filled sphere. For the 0.5 mm air-filled sphere the target strength for continuous tones is relatively constant, but has excursions at regular intervals, especially below 200 kHz. Excursions also occur for chirps with a bandwidth of 1 kHz and pulse lengths longer than 500 μs. The 2 mm air-filled sphere also has the excursions, which for pulsed signals extend to the highest frequencies calculated. However, the most prominent feature is a broad peak centred on 165 kHz, for which the target strengths reach 10 dB above the mean value elsewhere. The 5 mm air-filled sphere shows similar features, with the excursions more frequent and intense, and the broad peak centred on 58 kHz. For the 10 mm air-filled sphere the mean target strength is a few dB higher and fluctuates, and the excursions are more frequent and intense. They are quite periodic, in common with Figure 5 of Hickling (1964). The broad peak is less intense and now centred on 27 kHz, and another broad peak some 5 dB above the nearby mean target strength has appeared at 268 kHz.

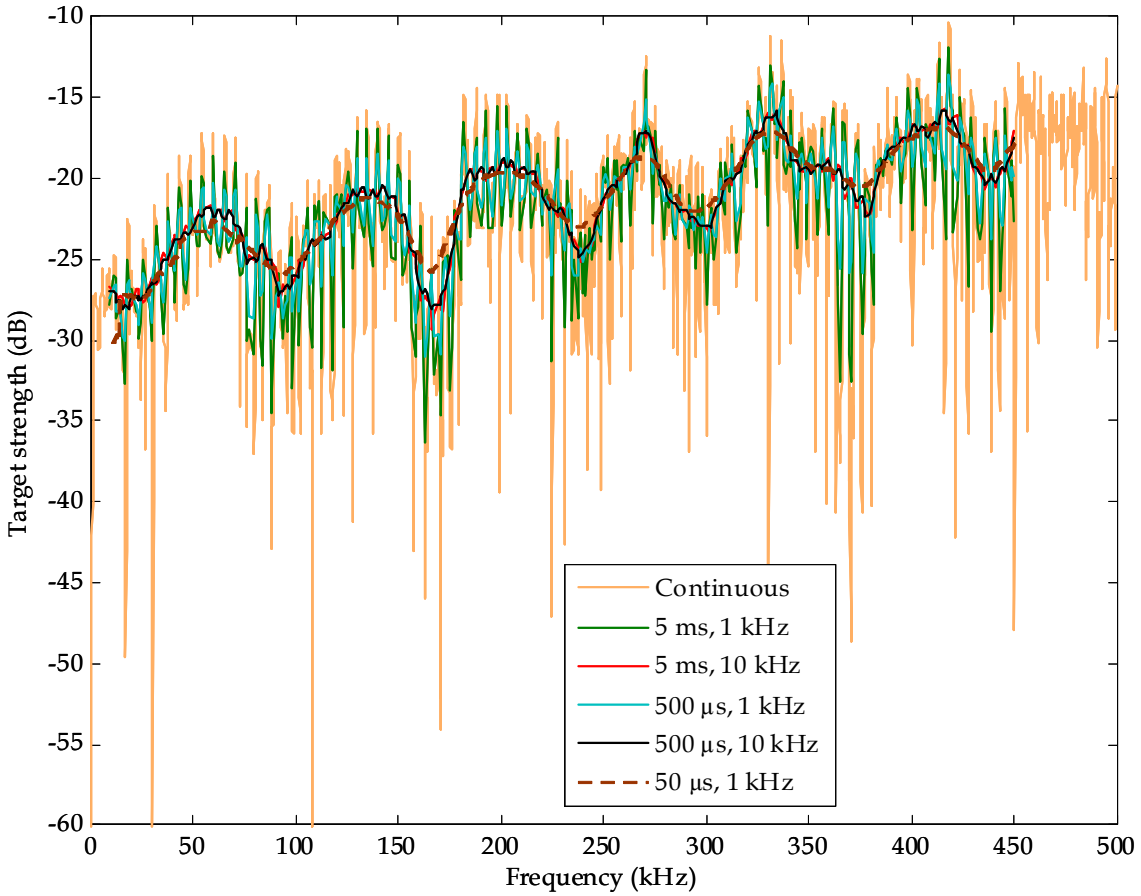


*Figure 13: Target strength of a solid sphere for continuous tones and for 1 and 10 kHz bandwidth hyperbolic frequency modulated chirps of 50 µs, 500 µs and 5 ms duration.*

Two distinct features of air-filled spheres are to be noted. The regularly spaced excursions evident with continuous tone ensonification are due to Lamb waves propagating on the surface of the shell (Gaunaurd and Werby, 1991). These narrow resonances also occur for chirps of relatively narrow bandwidth, and for all but the shortest duration. They lead to a significant variation of target strength with small changes of frequency. The variation becomes more extreme as the wall thickness increases. Care should therefore be exercised when using such a target to assess the range detection performance of a sonar that switches between closely spaced frequency bins. If the target strength is (incorrectly) assumed constant, the detection range will appear to vary significantly between the frequency bins.

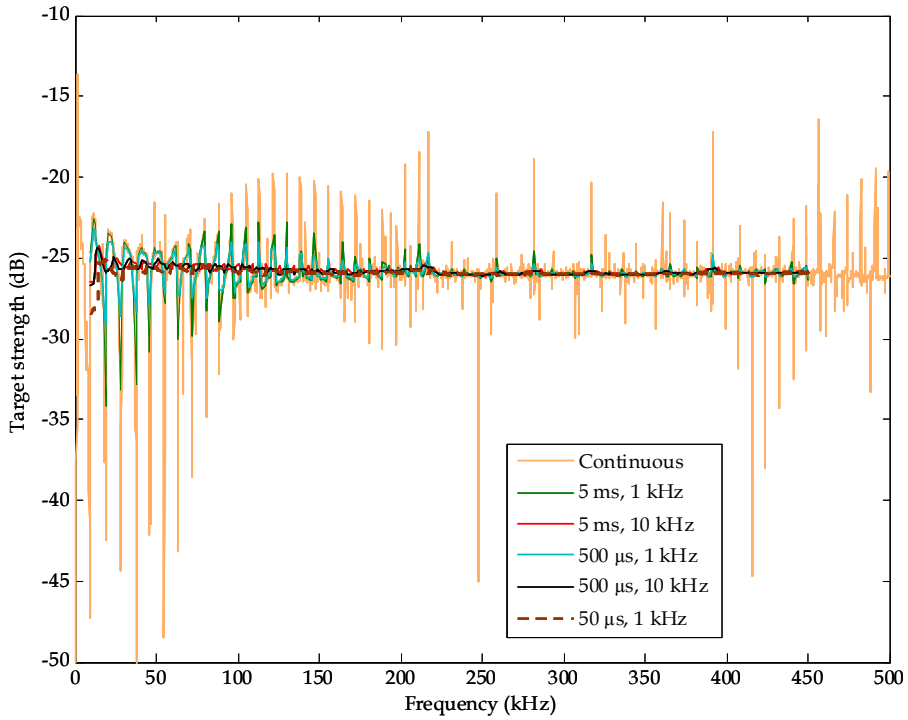


*Figure 14: Target strength of an air-filled stainless steel spherical shell of 20 cm diameter and 0.5 mm wall thickness for continuous tones and for 1 and 10 kHz bandwidth hyperbolic frequency modulated chirps of 50 µs, 500 µs and 5 ms duration.*

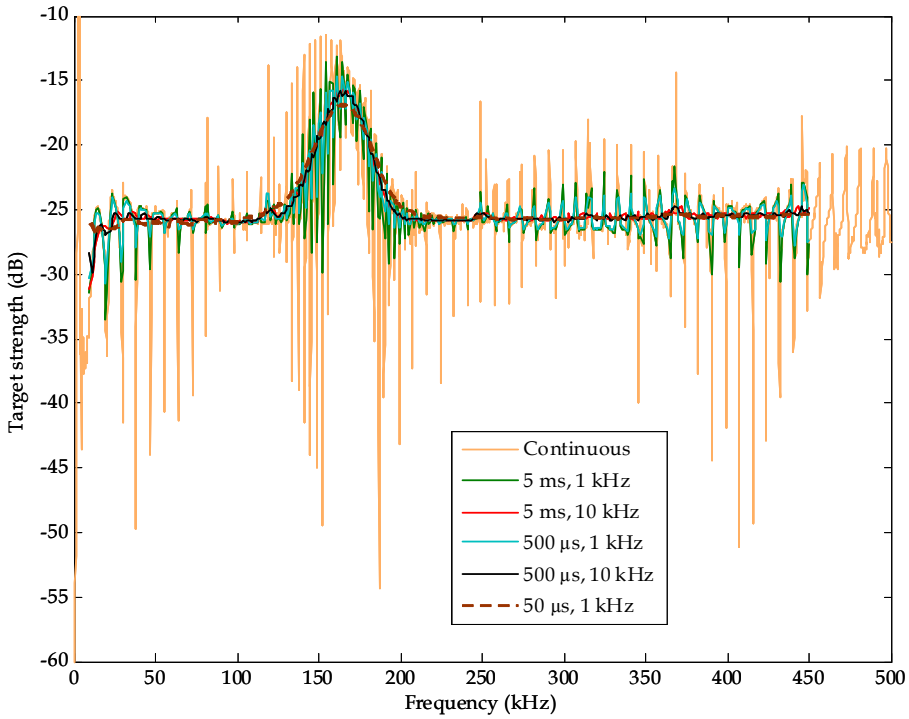


*Figure 15: Target strength of an air-filled stainless steel spherical shell of 20 cm diameter and 2 mm wall thickness for continuous tones and for 1 and 10 kHz bandwidth hyperbolic frequency modulated chirps of 50 µs, 500 µs and 5 ms duration.*

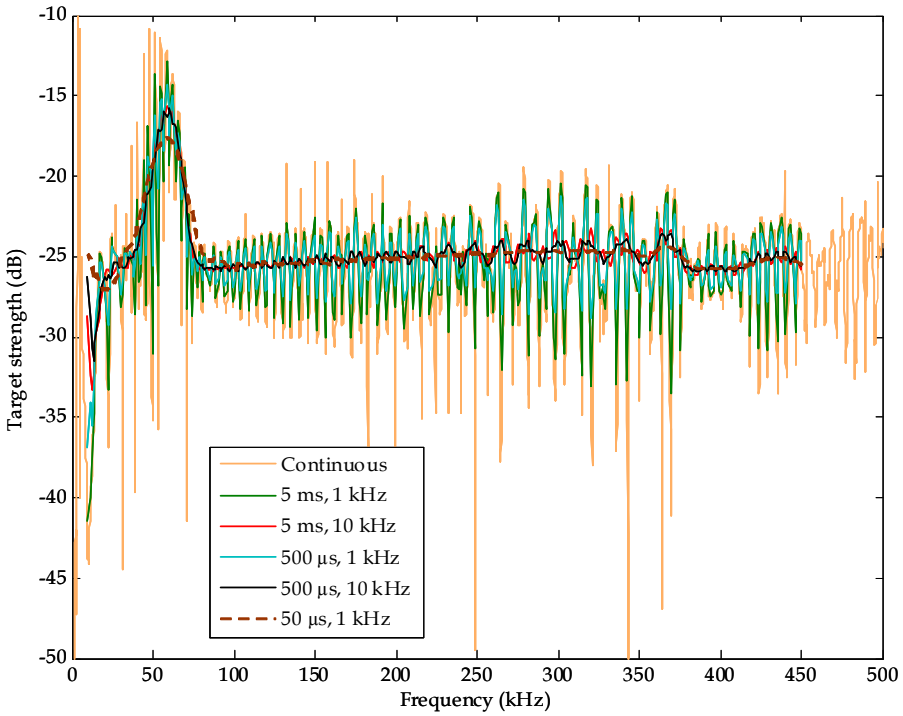


*Figure 16: Target strength of an air-filled stainless steel spherical shell of 20 cm diameter and 5 mm wall thickness for continuous tones and for 1 and 10 kHz bandwidth hyperbolic frequency modulated chirps of 50 µs, 500 µs and 5 ms duration.*

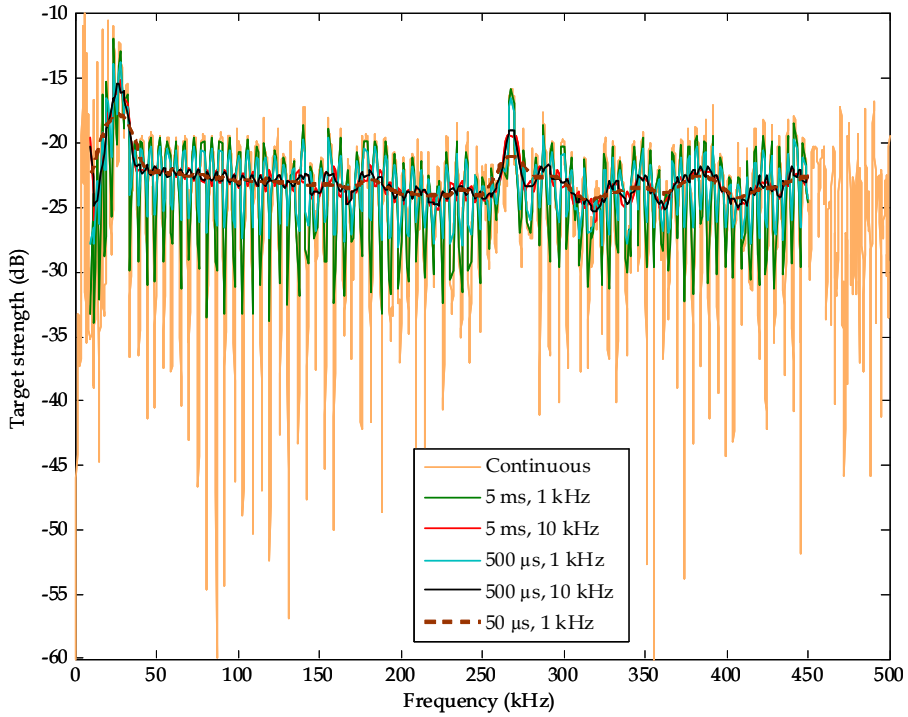


*Figure 17: Target strength of an air-filled stainless steel spherical shell of 20 cm diameter and 10 mm wall thickness for continuous tones and for 1 and 10 kHz bandwidth hyperbolic frequency modulated chirps of 50 µs, 500 µs and 5 ms duration.*

The broad peaks observed for the 2, 5 and 10 mm air-filled spheres are resonances due to flexural waves. They occur near what is termed the "coincidence frequency", when the phase velocity of the flexural waves in the shell is about equal to the speed of sound in the ambient water. Werby found that the Mindlin – Timoshenko thick plate theory (Ross, 1976) was quite reliable in predicting the phase velocity for the curved surfaces of thin spherical shells. Equations for the phase velocity are given in Ross (1976), and repeated in a series of papers by Werby and colleagues (e.g., Werby, 1990; Werby and Gaunaurd, 1991; Werby and Chin-Bing, 1991; Werby and Gaunaurd, 1992). On the low frequency shoulders of these broad resonance peaks, there are a series of narrow resonances known as "leaky pseudo-Stoneley resonances" or "Junger-type resonances" (Gaunaurd and Werby, 1991). They are due to a surface wave which occurs at the interface of an elastic plate which is fluid-loaded on only one side.

Previous studies of these various resonances have usually only considered continuous tones as the exciting source. When narrow bandwidth chirps are used, all resonances are present. When wide bandwidth chirps are used, the Lamb and Junger-type resonances are not evident, however, the flexural resonance remains.

Next, the variation of target strength with pulse length and bandwidth is considered. Selecting a frequency of 100 kHz and bandwidth of 10 kHz, the variation of target strength with the pulse length of the hyperbolic frequency modulated chirp is shown in Figure 18 for a fluid-filled, solid and 5 mm air-filled sphere. The variations are generally small, with the target strength contained within a band of 0.4 dB for the fluid-filled sphere and 0.6 dB for the other targets. The variations for the solid sphere might be expected from the experimental measurements of Hampton and McKinney (1961) on solid metal spheres.

In Figure 19, target strengths have been calculated for the same targets with hyperbolic frequency modulated chirps of 500 μs duration, with bandwidths of up to 50% of the centre frequency. The centre frequency in this case was 100 kHz. Again the target strength of the fluid-filled sphere is fairly constant. The 5 mm air-filled sphere shows a modest increase of 1 dB in the target strength as the bandwidth increases to 15 kHz, but remains fairly constant for larger bandwidths. The solid sphere shows a similar variation over a broader range of bandwidths, but generally an increase of the target strength with increasing bandwidth.

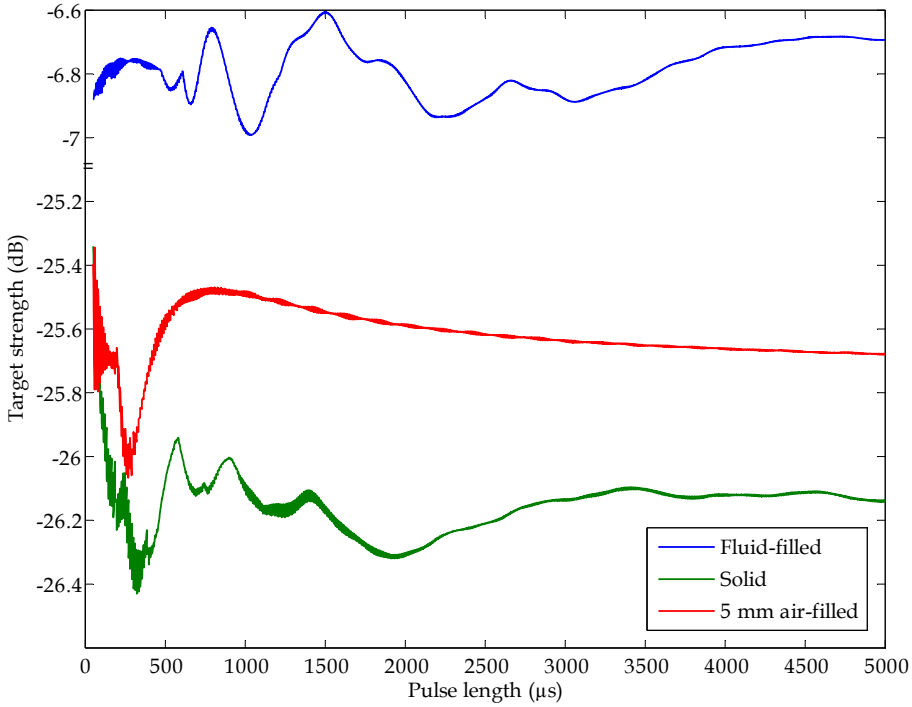


*Figure 18: Target strength of fluid-filled, solid and 5 mm air-filled spheres. The targets are exposed to hyperbolic frequency-modulated chirped waveforms of 10 kHz bandwidth centred on 100 kHz, with pulse lengths between 50 μs and 5 ms. Note the break in the ordinate axis.*

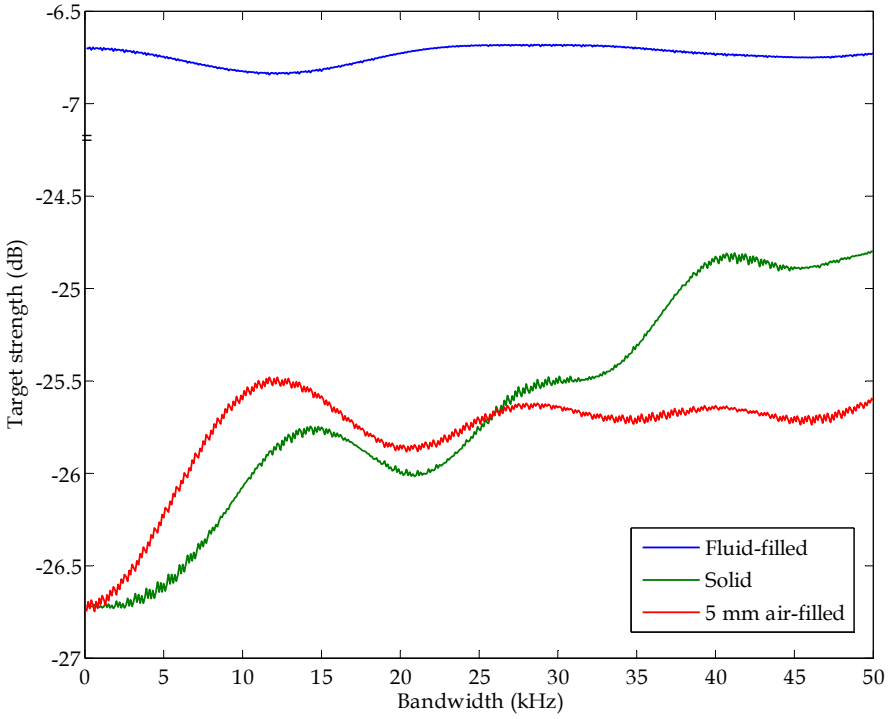


*Figure 19: Target strength of fluid-filled, solid and 5 mm air-filled spheres. The targets are exposed to hyperbolic frequency-modulated chirped waveforms of 500 μs duration, with the indicated bandwidth centred on 100 kHz. Note the break in the ordinate axis.*

## 3.2 Signals in the time domain

Figures 20 to 25 show the reflected signal in the time domain, where 0 ms corresponds to the arrival of the first portion of the reflected signal at the receiver. The pressure is relative to a value of 1 at the projector. In Figures 20 to 22 the waves impinge upon a fluid-filled sphere. Overlain in Figure 20 are the reflected signals when the projector emits hyperbolic frequency modulated chirps of 1 kHz bandwidth centred on 100 kHz, and of 50 μs, 500 μs and 5 ms duration. Returns separated in time are most clearly seen for the shorter pulses. The most intense signal corresponds to the focused reflection from the rear of the sphere, which arrives 0.47 ms after the specular reflection from the front surface. Subsequent reflections are related to multiple internal reflections within the sphere. As the duration of the impinging signal increases, there is overlap of signals returning from different parts of the sphere, but that from the rear surface still dominates. The same comments apply to Figures 21 and 22, where the bandwidth is increased to 10 and 50 kHz, respectively. However the longest duration chirps result in quite complex returns.

As a comparison, Figures 23 to 25 show the reflected signals from a solid and a 5 and 10 mm air-filled sphere, respectively. For each target the projector emitted hyperbolic frequency modulated chirps of 50 kHz bandwidth centred on 100 kHz, and of 50 μs, 500 μs and 5 ms duration. For the solid spherical target, the strong specular return from the front surface dominates the reflected signal for the shortest-duration chirp. However, for chirps whose duration is long compared to the transit time across the sphere, the superposition of reflected signals leads to a complex return. For the air-filled spheres the strong specular reflection is followed by a wave traversing the water and coupling into the thick shell material, travelling circumferentially around it and being emitted back into the water in the direction of the receiver. This second return is stronger for the sphere with the thicker shell. It commences approximately 180 μs after the start of the specular return, and since the specular return lasts 500 μs, it is superposed upon it, leading to periodic doubling and zeroing of the magnitude of the pressure with time.

Comparing all the returns in the time domain, if no further signal processing is employed, there is an advantage in using short pulses to elucidate details of the target's structure, but little is gained by increasing the bandwidth of the transmitted signal.

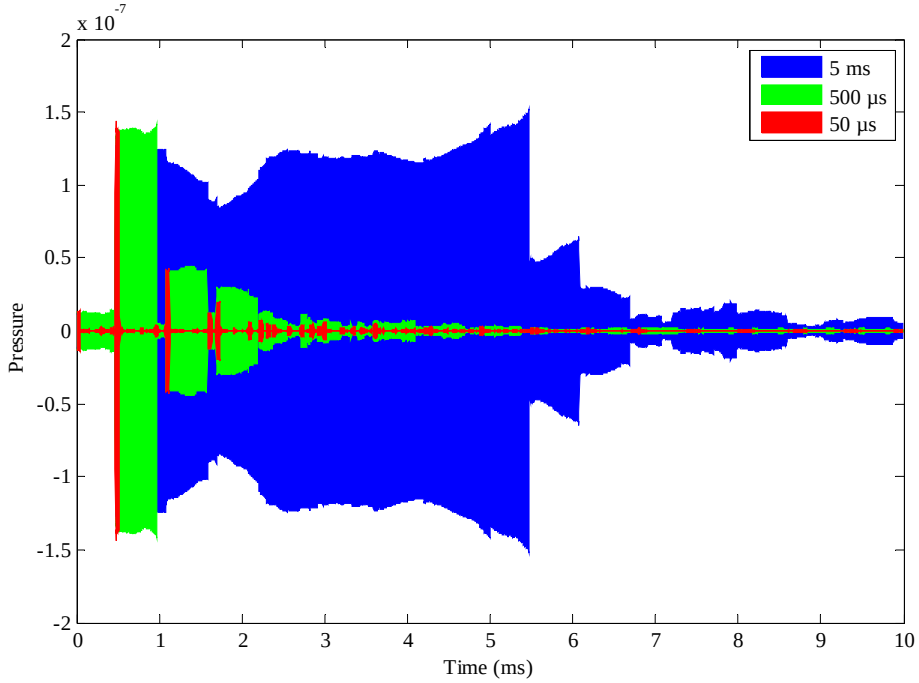


*Figure 20: The reflected signal arriving at the receiver from a fluid-filled sphere. The projector emitted 1 kHz bandwidth hyperbolic frequency modulated chirps centred on 100 kHz and of 50 µs, 500 µs and 5 ms duration.*

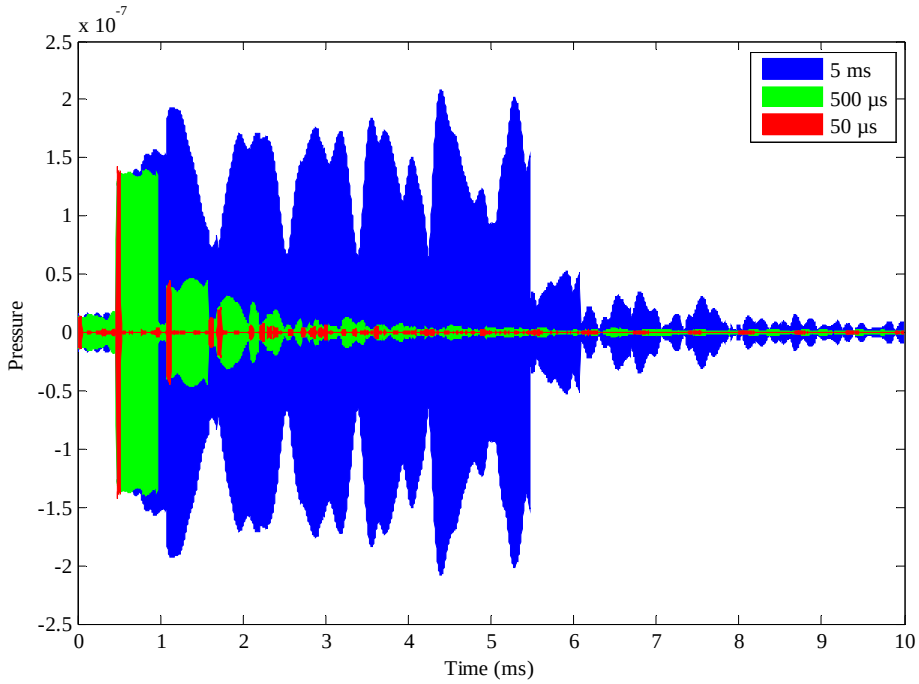


*Figure 21: The reflected signal arriving at the receiver from a fluid-filled sphere. The projector emitted 10 kHz bandwidth hyperbolic frequency modulated chirps centred on 100 kHz and of 50 µs, 500 µs and 5 ms duration.*

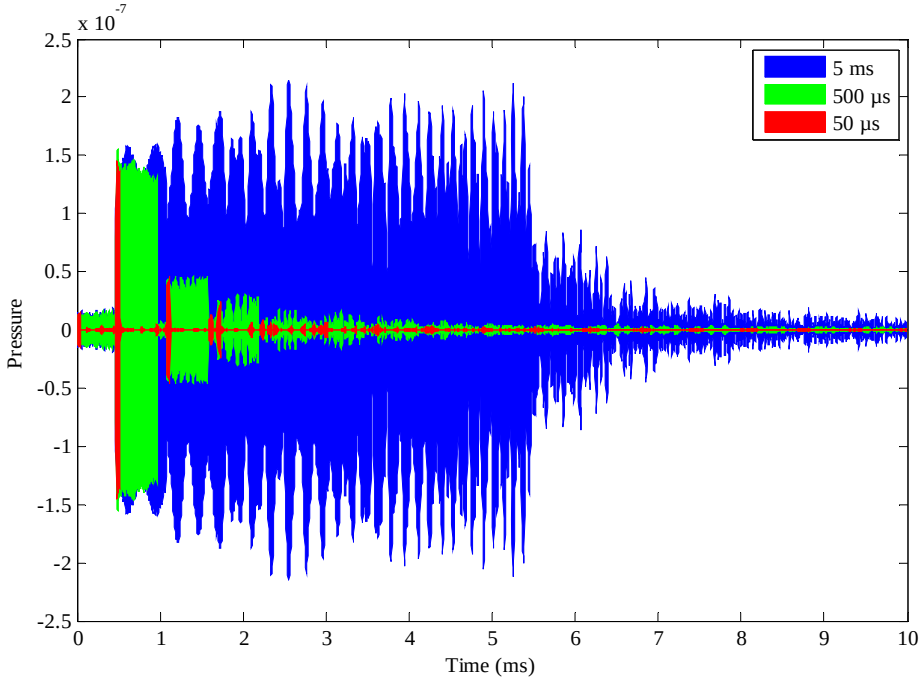


*Figure 22: The reflected signal arriving at the receiver from a fluid-filled sphere. The projector emitted 50 kHz bandwidth hyperbolic frequency modulated chirps centred on 100 kHz and of 50 µs, 500 µs and 5 ms duration.*

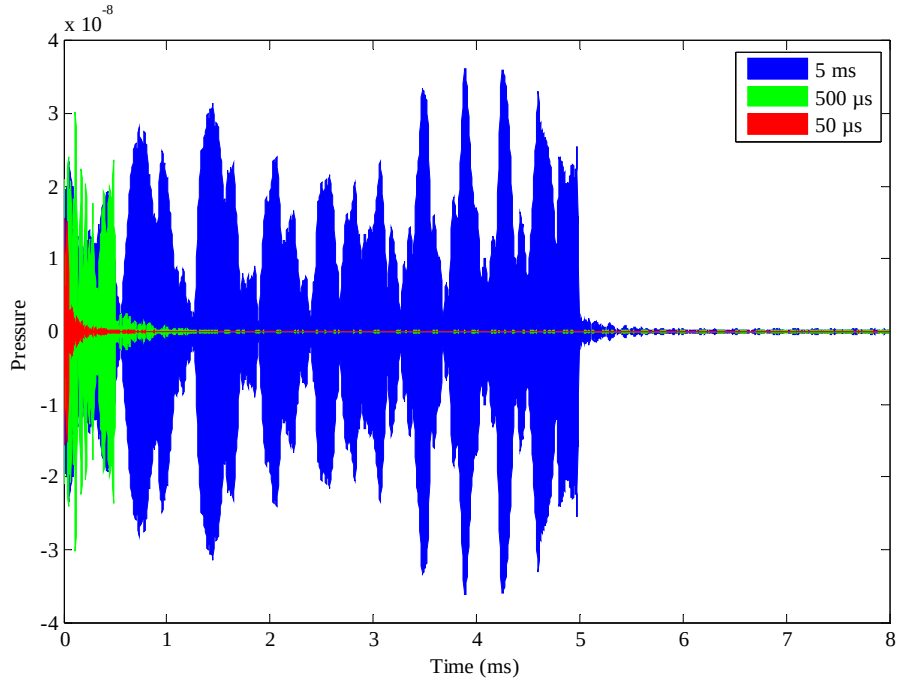


*Figure 23: The reflected signal arriving at the receiver from a solid sphere. The projector emitted 50 kHz bandwidth hyperbolic frequency modulated chirps centred on 100 kHz and of 50 µs, 500 µs and 5 ms duration.*

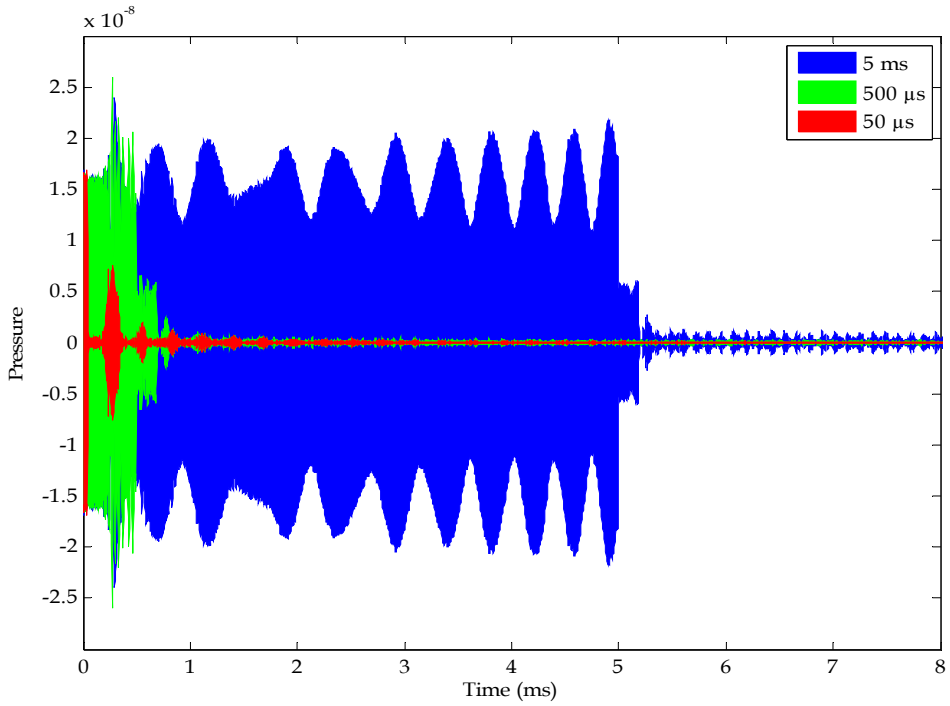


*Figure 24: The reflected signal arriving at the receiver from a 5 mm air-filled sphere. The projector emitted 50 kHz bandwidth hyperbolic frequency modulated chirps centred on 100 kHz and of 50 µs, 500 µs and 5 ms duration.*

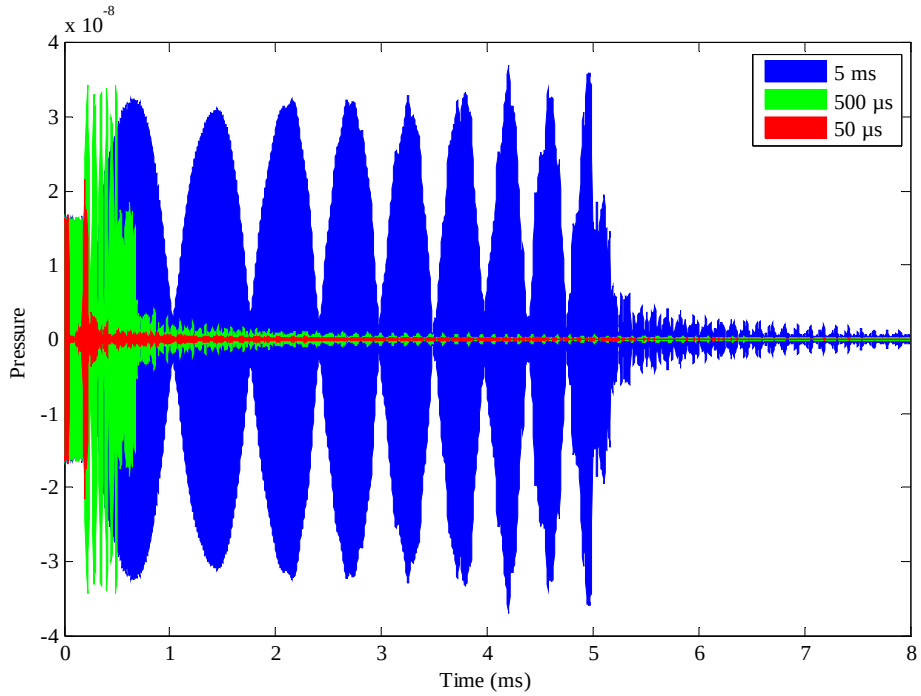


*Figure 25: The reflected signal arriving at the receiver from a 10 mm air-filled sphere. The projector emitted 50 kHz bandwidth hyperbolic frequency modulated chirps centred on 100 kHz and of 50 µs, 500 µs and 5 ms duration.*

## 3.3 Matched filter processing

However, to improve the detection performance of a sonar, almost certainly some signal processing will be attempted. The effect of signal processing is not included in the target strength parameter of the sonar equation, but incorporated in the detection threshold parameter. Dawe (1997) shows how different detection and signal processing techniques affect this latter parameter. In one common signal processing technique, a replica of the outgoing waveform is used in a matched filtering process for detection. The transmitted signal is cross-correlated with the reflected signal, and a sharp peak in the correlation occurs at the temporal location of the main return from the target. Other returns from the target lead to further peaks in the correlation.

The result of such a correlation is considered in Figures 26 and 27 for a fluid-filled sphere. In Figure 26, the effect of changing the duration of a hyperbolic frequency modulated chirped pulse is shown for a waveform with a bandwidth of 10 kHz centred on 100 kHz. For a 50 µs pulse the strongest correlation coincides with the return from the rear of the sphere. As the pulse length increases this reflection provides the strongest correlation, but the complex return results in other strong correlations. Figure 27 shows the effect of changing the bandwidth for a pulse of 500 µs duration. Increasing the bandwidth leads to a sharper correlation, and hence, increased range resolution.

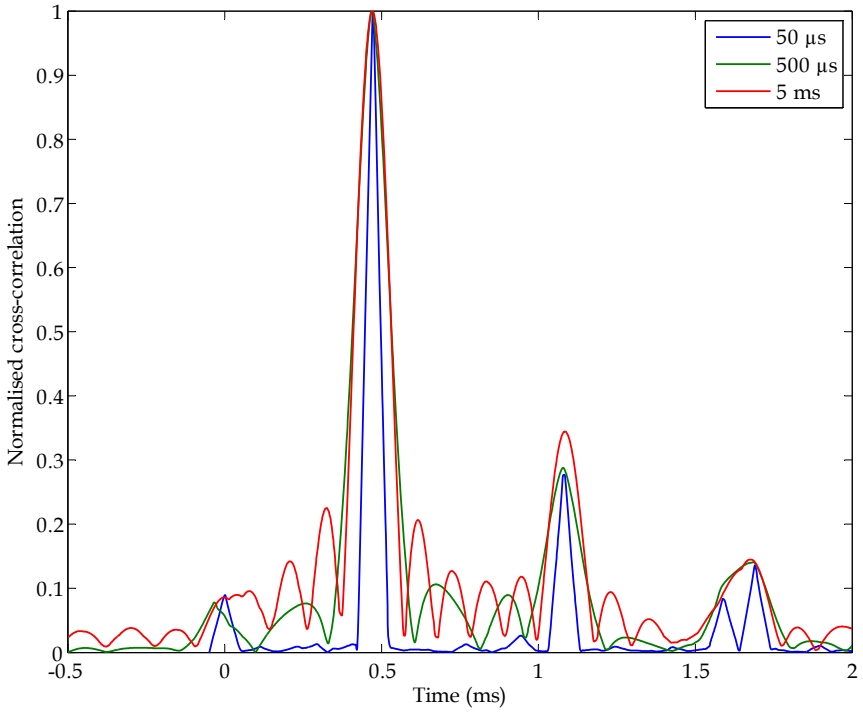


*Figure 26: The normalised envelope of the cross-correlation between a replica of the signal sent from a projector and the signal arriving at a receiver from a fluid-filled sphere. The projector emitted 10 kHz bandwidth hyperbolic frequency modulated chirps centred on 100 kHz and of 50 µs, 500 µs and 5 ms duration.*

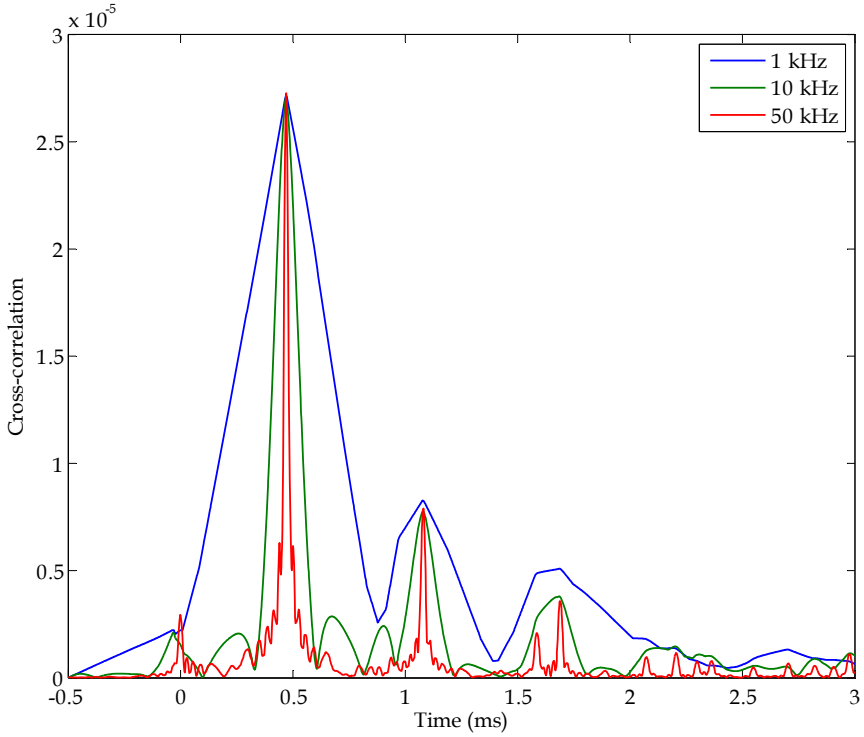


*Figure 27: The envelope of the cross-correlation between a replica of the signal sent from a projector and the signal arriving at a receiver from a fluid-filled sphere. The projector emitted 500 µs hyperbolic frequency modulated chirps with bandwidths of 1, 10 and 50 kHz centred on 100 kHz.*

Comparison is made in Figures 28 and 29 of the effect of bandwidth on the correlation for a solid and a 10 mm air-filled sphere, respectively. The transmitted signal is of 500 µs duration, with bandwidths of 1, 10 and 50 kHz, centred on 100 kHz. For both targets, the correlation sharpens with increased bandwidth, but in neither case is the correlation as sharp as for the fluid-filled sphere.

The sharpness of the correlation of the most intense peak is shown in Figure 30. The full width at half maximum of the envelope of this peak is plotted as a function of bandwidth for a fluid-filled, a solid and a 10 mm air-filled sphere. The transmitted signal is of 500 µs duration, with bandwidths of 1 to 50 kHz centred on 100 kHz. The steps at 11 and 29 kHz for the 10 mm air-filled and solid targets are due to the resolution of a broad peak into two narrower component peaks. The inset plots the same data on logarithmic axes, and clearly shows the inverse relationship between bandwidth and temporal resolution above a bandwidth of several kilohertz. Below a bandwidth of 10 kHz, the fluid-filled sphere has the sharpest correlation, but above 30 kHz there is little difference between the three targets.

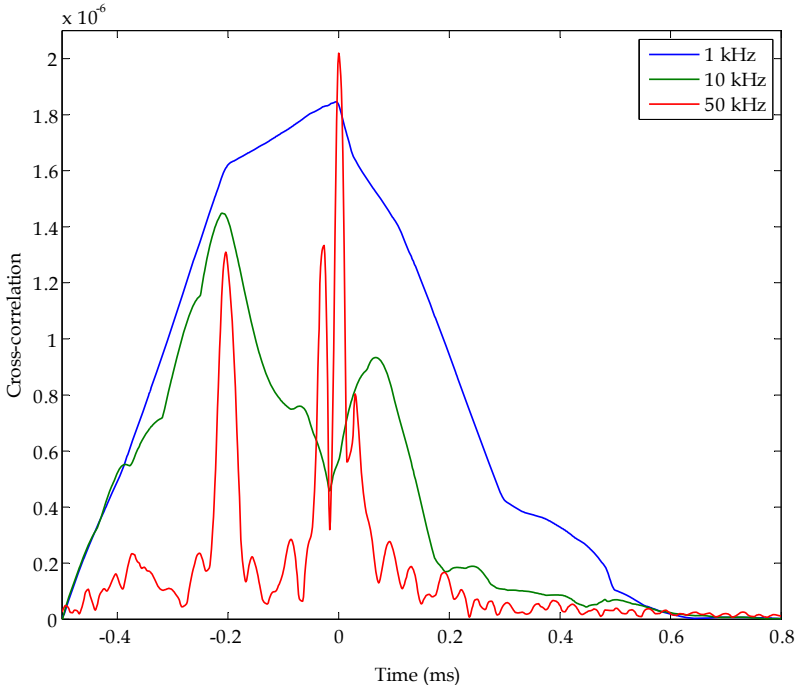


*Figure 28: The envelope of the cross-correlation between a replica of the signal sent from a projector and the signal arriving at a receiver from a* **solid sphere**. *The projector emitted 500 µs hyperbolic frequency modulated chirps with bandwidths of 1, 10 and 50 kHz centred on 100 kHz.*

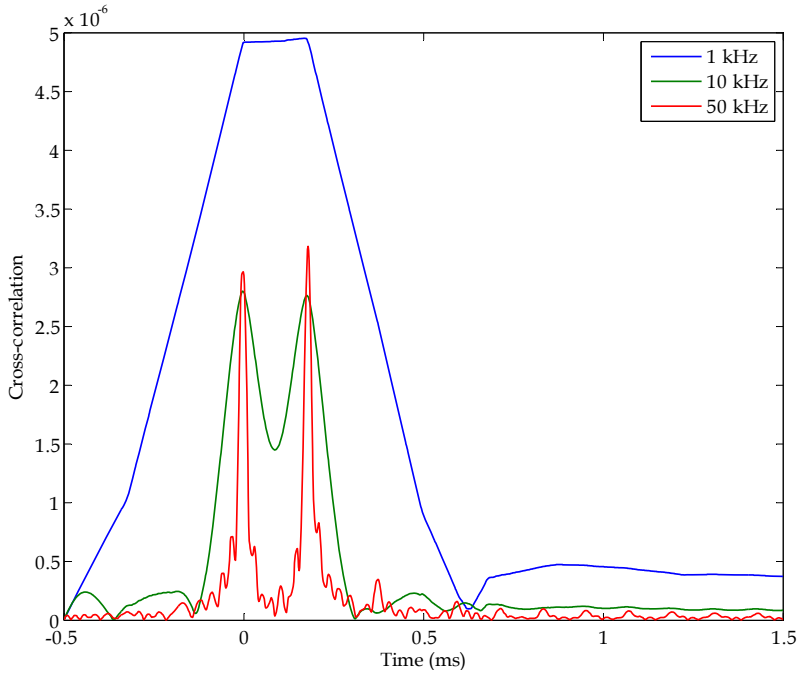


*Figure 29: The envelope of the cross-correlation between a replica of the signal sent from a projector and the signal arriving at a receiver from a* **10 mm air-filled sphere**. *The projector emitted 500 µs hyperbolic frequency modulated chirps with bandwidths of 1, 10 and 50 kHz centred on 100 kHz.*

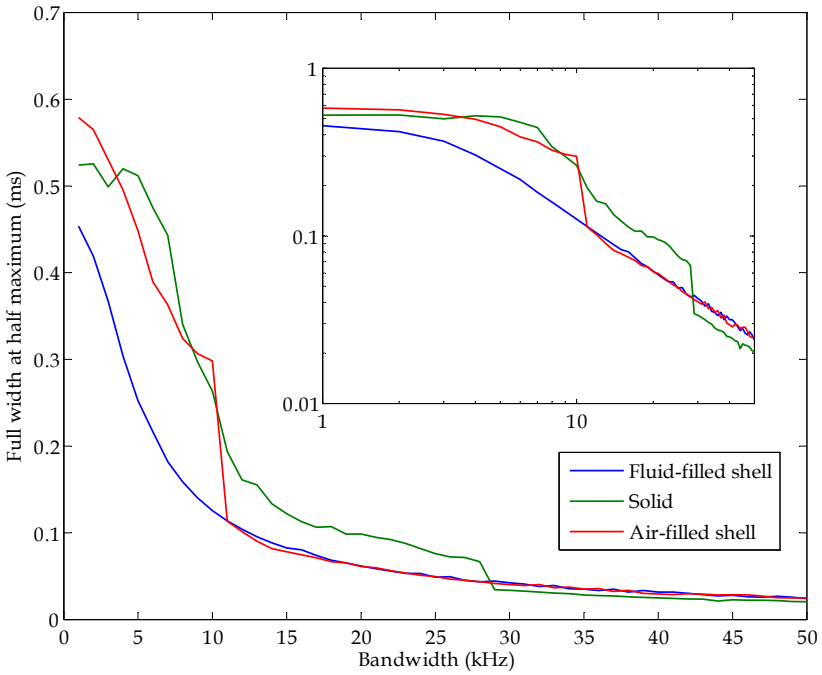


*Figure 30: The full width at half maximum of the most intense peak in the envelope of the correlation between a replica of the signal sent from a projector and the signal arriving at a receiver. The targets are a fluid-filled, solid and 10 mm air-filled sphere. The targets are exposed to hyperbolic frequency-modulated chirped waveforms of 500 µs duration, with the indicated bandwidth centred on 100 kHz. The inset shows the same data on logarithmic axes.*

Figures 31 and 32 compare the envelopes of the return signals and replicate cross-correlations for 500 µs hyperbolic frequency modulated chirps with bandwidths of 10 and 50 kHz, respectively, centred on 100 kHz. The target is the fluid-filled sphere. The start of each partial wave is clearly shown by a spike in the cross-correlation, but the details of the partial wave are lost. These results are expected as cross-correlation using chirped signals leads to pulse compression. In Figure 33, the bandwidth is 50 kHz and the target is the 10 mm air-filled sphere. The start of the specular return and circumferentially travelling wave are clearly seen in the cross-correlation, but details of the superposition of the two between 180 and 500 µs are absent. This is a region where the phase of the return signal is changing rapidly, as seen in Figure 34, which plots the pressure envelope, and the phase difference between the return and replicate of the transmitted signal over this time period. Also note that the nulls in the pressure correspond to the most rapid phase changes.

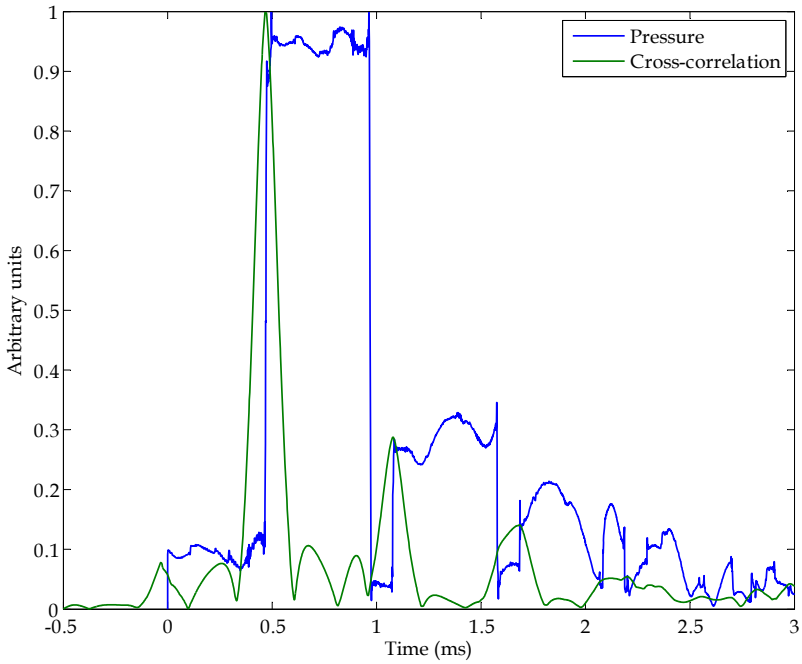


*Figure 31: The envelope of the reflected signal arriving at the receiver from a fluid-filled sphere, and the envelope of the cross-correlation between it and a replica of the signal sent from a projector. The projector emitted 500 µs hyperbolic frequency modulated chirps with a bandwidth of 10 kHz centred on 100 kHz.*

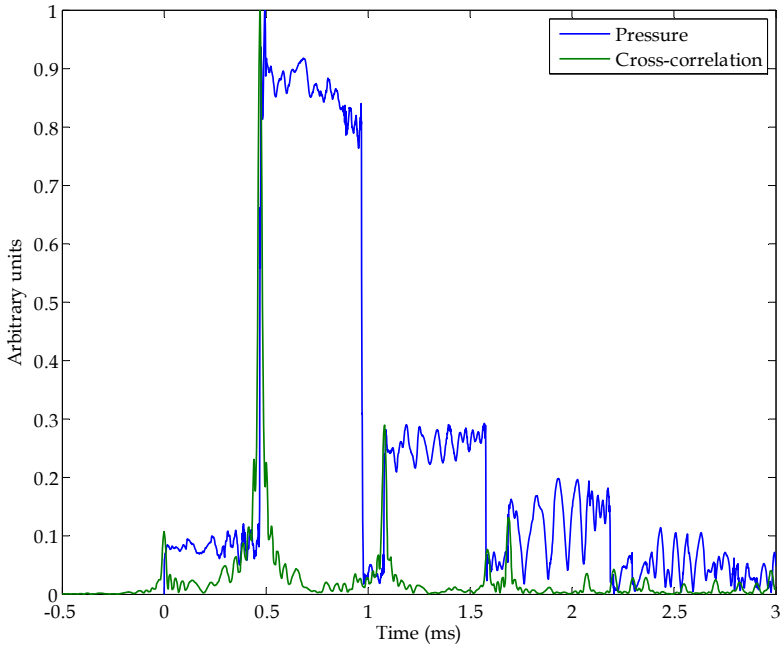


*Figure 32: The envelope of the reflected signal arriving at the receiver from a fluid-filled sphere, and the envelope of the cross-correlation between it and a replica of the signal sent from a projector. The projector emitted 500 µs hyperbolic frequency modulated chirps with a bandwidth of 50 kHz centred on 100 kHz.*

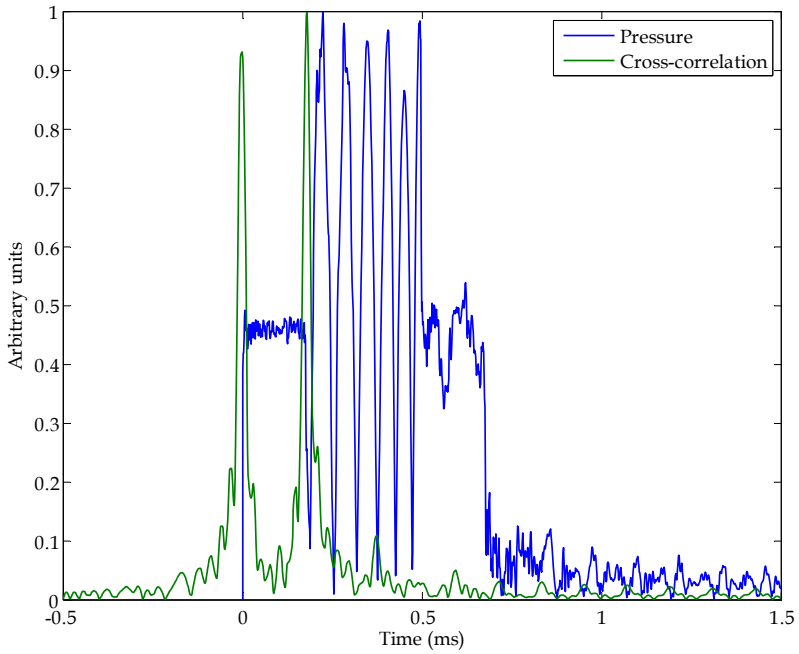


*Figure 33: The envelope of the reflected signal arriving at the receiver from a 10 mm air-filled sphere, and the envelope of the cross-correlation between it and a replica of the signal sent from a projector. The projector emitted 500 µs hyperbolic frequency modulated chirps with a bandwidth of 50 kHz centred on 100 kHz.*

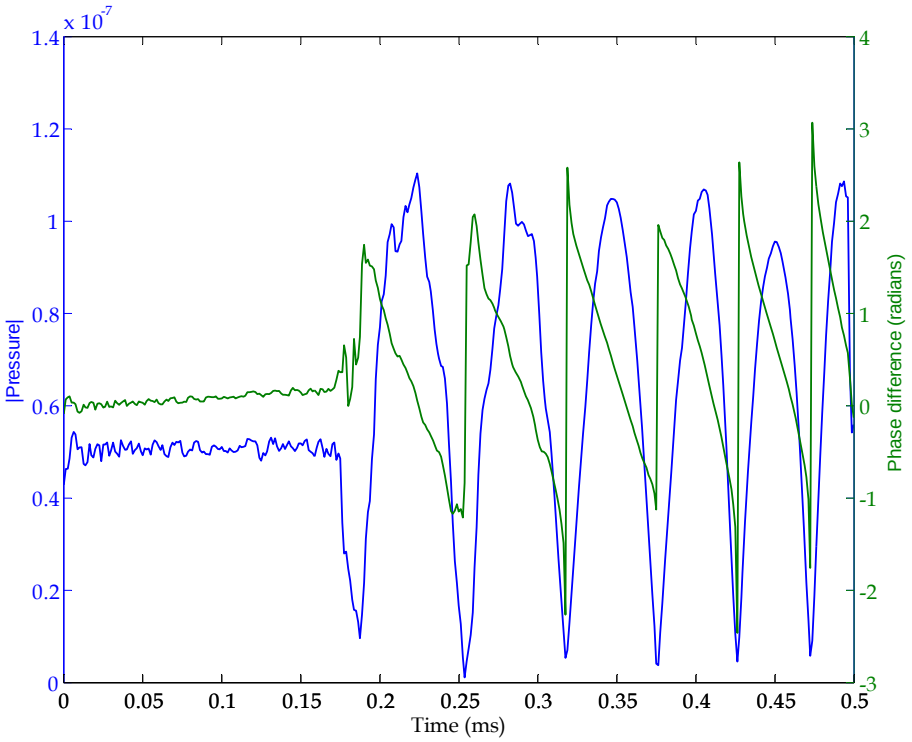


*Figure 34: The first 500 µs of the envelope of the reflected signal arriving at the receiver from a 10 mm air-filled sphere, and the phase difference between it and a replica of the signal sent from a projector. The projector emitted 500 µs hyperbolic frequency modulated chirps with a bandwidth of 50 kHz centred on 100 kHz.*

## 3.4 Temperature variations

Attention is now given to the effect of temperature on target strength. For most targets the effect is negligible, as, for example, shown in Figure 35, which plots the target strength of a 5 mm air-filled sphere as a function of frequency for water temperatures of 20 and 30°C. However, as noted in Readhead (*op. cit.*) a fluid-filled sphere does exhibit considerable variation of the target strength with temperature. This is because the focusing effect of the fluid-filling is sensitive to the refractive index, which changes with temperature. The extent is quantified in the following figures, all of which refer to the fluid-filled sphere.

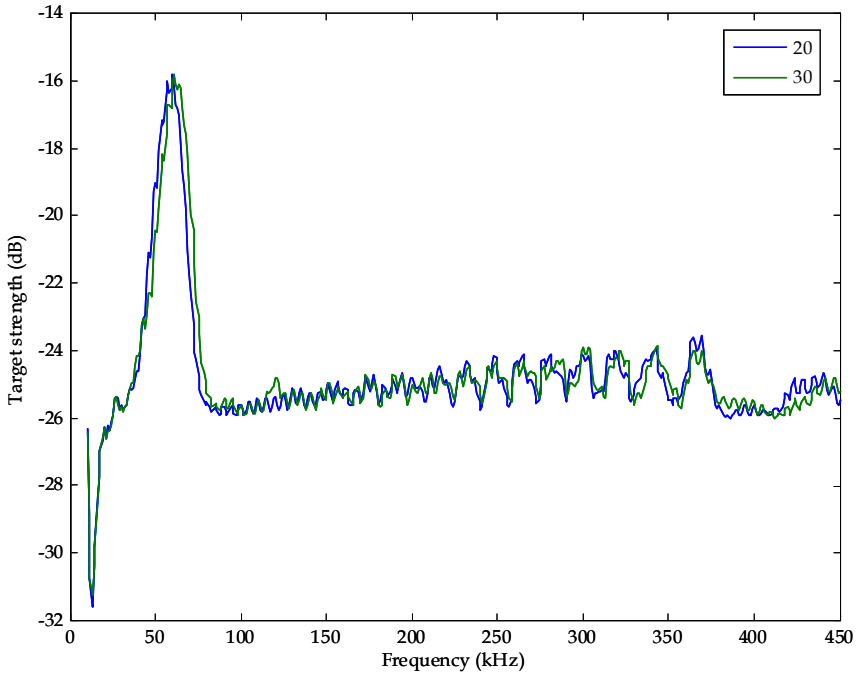


*Figure 35: Variation of target strength with frequency for a 5 mm air-filled sphere deployed in sea water of 20 and 30°C. The incoming waves are 10 kHz bandwidth hyperbolic frequency modulated chirps of 500 µs duration.*

Figures 36 and 37 display the target strength as a function of frequency to 450 kHz for water temperatures of 5, 10, 15, 20, 25, 30 and 35°C. It is assumed that the water and internal fluid have reached thermal equilibrium. In Figure 36 the projector emits 5 ms hyperbolic frequency modulated chirps of 10 kHz bandwidth. In Figure 37 the bandwidth is 10% of the centre frequency. The same variability as in Figure 5 is seen in Figure 36. In Figure 37 the variability falls with increasing frequency, due to the increasing bandwidth (in comparison to Figure 36), but the overall trends are similar. From both figures it can be seen that at frequencies above 200 kHz, the behaviour of the target strength for water temperatures above and below 20°C is quite different. Below 20°C the target strength generally increases with frequency; whereas above 20°C it decreases.

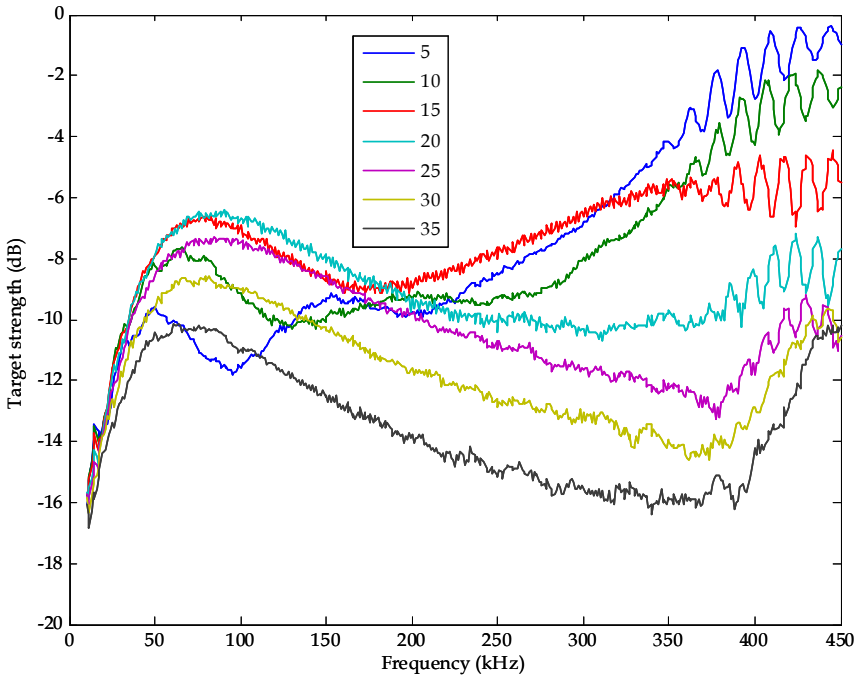


*Figure 36: Variation of target strength with frequency for a fluid-filled sphere at 5, 10, 15, 20, 25, 30 and 35°C. The incoming waves are 10 kHz bandwidth hyperbolic frequency modulated chirps of 5 ms duration.*

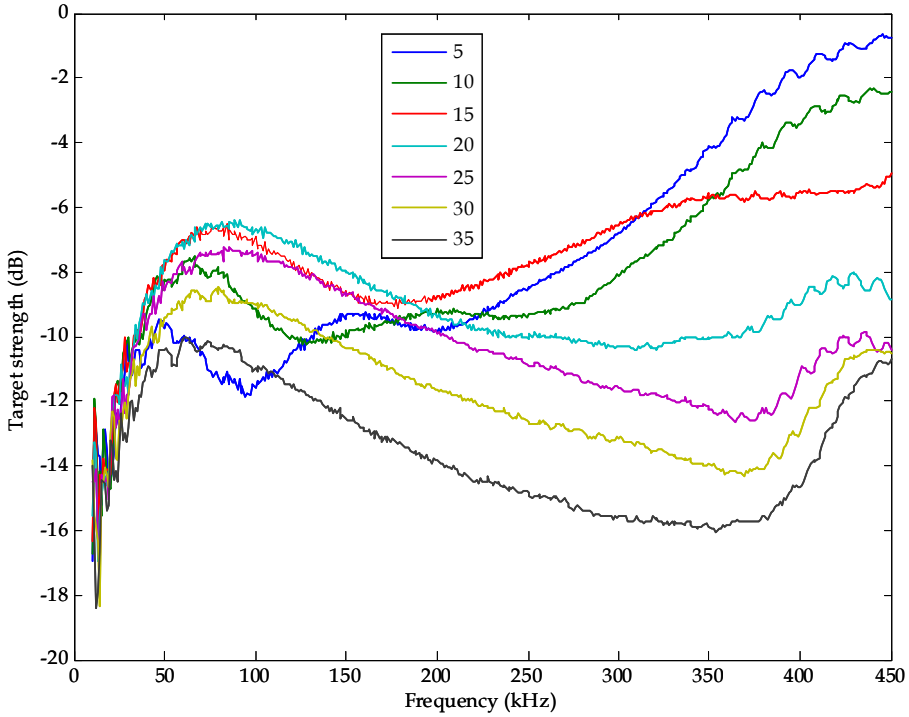


*Figure 37: Variation of target strength with frequency for a fluid-filled sphere at 5, 10, 15, 20, 25, 30 and 35°C. The incoming waves are hyperbolic frequency modulated chirps of 5 ms duration with bandwidths of 10% of the centre frequency.*

Similar data are presented in a different manner in Figure 38, where target strength is plotted as a function of water temperature for centre frequencies from 50 to 450 kHz in 50 kHz steps. In this case, the projector emits 500 μs hyperbolic frequency modulated chirps with bandwidths of 10% of the centre frequency. Below 200 kHz, the target strength does not vary by more than a few decibels over this wide temperature range. The maximum target strength is attained at a temperature of about 20°C, and decreases as the temperature departs from this value. Above 300 kHz, the target strength generally decreases with increasing temperature, with a decline of more than 10 dB.

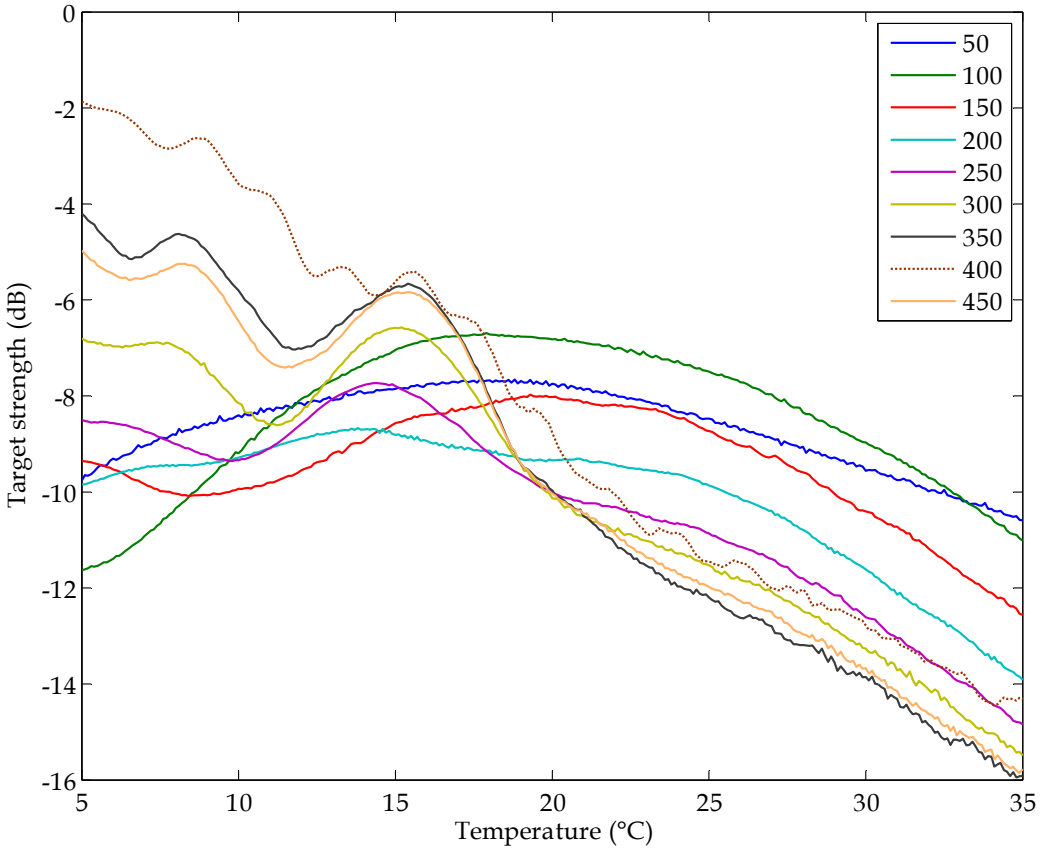


*Figure 38: Variation of target strength with temperature for a fluid-filled sphere. The incoming waves are hyperbolic frequency modulated chirps of 500 μs duration, with bandwidths of 10% centred on frequencies of 50, 100, 150, 200, 250, 300, 350, 400 and 450 kHz.*

Figure 39 plots the target strength for frequencies of 50, 100, 150 and 200 kHz between 15 and 25°C. The projector emits 500 μs hyperbolic frequency modulated chirps of 1 kHz bandwidth, a narrow bandwidth chosen to accentuate variations. However, the data demonstrate that if such a fluid-filled sphere is used within this temperature range at frequencies below 200 kHz, the target strength variation remains within a range of less than 1.5 dB.

However, the variability of target strength with temperature is in part due to the pulse type used, as might be expected from the data displayed in Figure 5. Figure 40 plots target strength versus water temperature for incoming waves of 1 and 10 kHz bandwidth hyperbolic frequency modulated chirps of 500 μs and 5 ms duration centred on 100 kHz. As might be expected small bandwidth signals of long duration produce great variability. For the other pulse types the variation of target strength with temperature is quite smooth and if water temperatures are restricted to a range of 15 – 25°C, the target strength varies by no more than 1 dB.

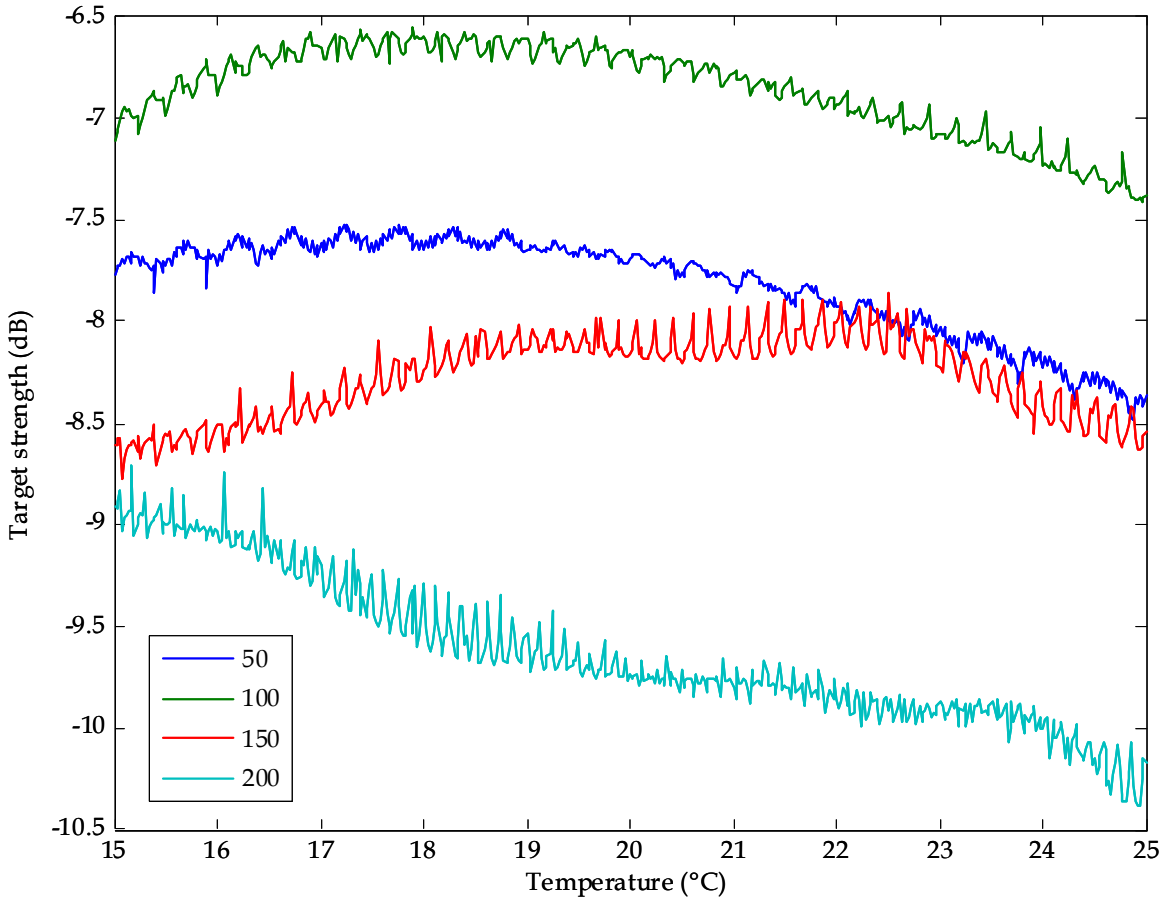


*Figure 39: Variation of target strength with temperature for a fluid-filled sphere. The incoming waves are 1 kHz bandwidth hyperbolic frequency modulated chirps of 500 μs duration centred on frequencies of 50, 100, 150 and 200 kHz.*

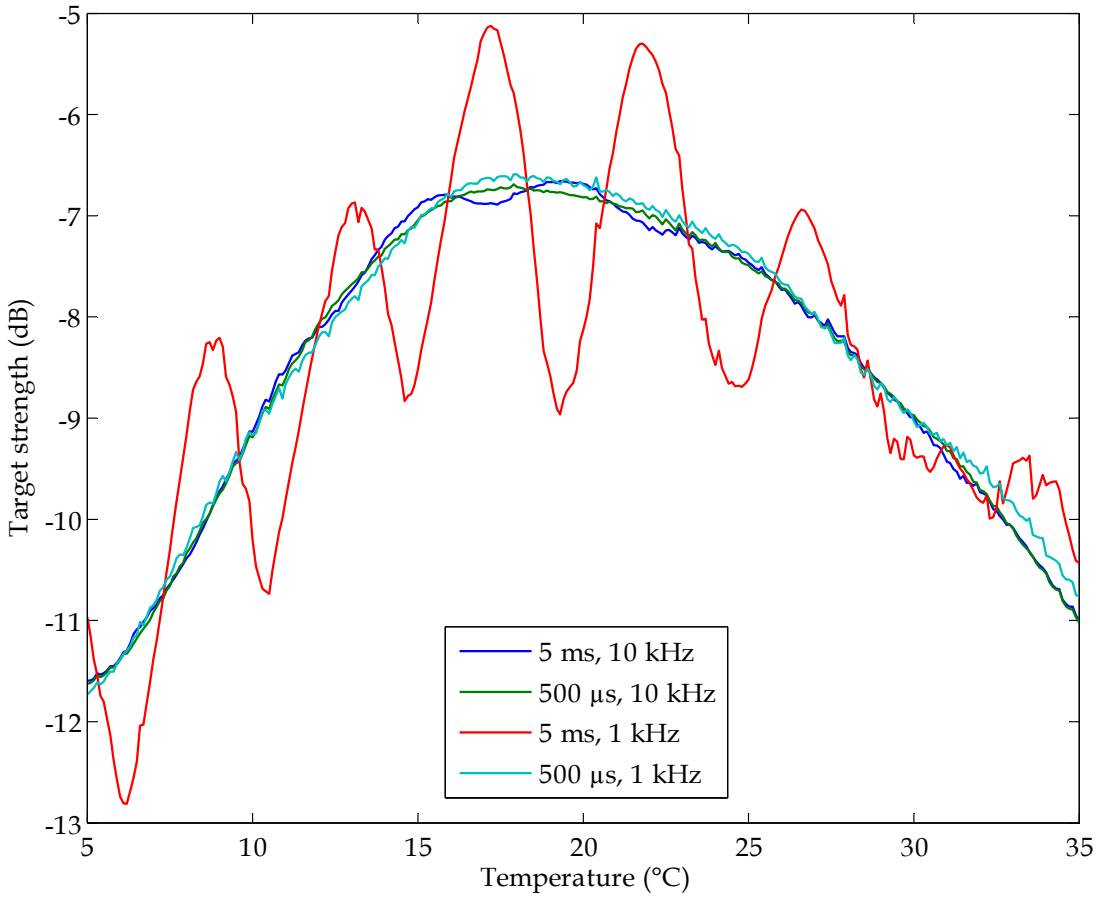


*Figure 40: Variation of target strength with temperature for a fluid-filled sphere. The incoming waves are 1 or 10 kHz bandwidth hyperbolic frequency modulated chirps of 500 µs and 5 ms duration centred on 100 kHz.*

# 4. Conclusion

Target strengths have been calculated for changes in frequency, pulse length, bandwidth and temperature for a fluid-filled sphere. Comparison has also been made with a solid sphere and air-filled spheres.

As seen in Readhead (*op. cit.*), the target strength of a fluid-filled sphere for continuous tones varies greatly with frequency, but for chirped pulses the variations are much less. Below 350 kHz, these variations are typically within a 0.4 dB wide band, but this band increases to as much as 4 dB for long chirps of narrow frequency bandwidth, such as 1 kHz. The solid and air-filled spheres show less variation for continuous tones, but in some cases, more variation for chirps. A solid sphere has target strength variations contained within a 1 dB wide band for wide bandwidth chirped pulses, but this band increases to 10 dB for narrow bandwidth chirps. For an air-filled sphere, these variations are sensitive to shell wall thickness. Typically they are contained within a 1 dB wide band, which increases to as much as 12 dB for narrow bandwidth chirps. Caution should then be used when interpreting results from a sonar which

switches between closely spaced frequency bins of narrow bandwidth to spatially resolve target returns.

However, unlike the solid and air-filled spheres, the target strength of a fluid-filled sphere does show sensitivity to ambient water temperature. As the temperature increases above 20°C, the target strength generally declines. As the temperature falls below 20°C the behaviour is mixed, with the target strength decreasing at frequencies below 200 kHz, and increasing at higher frequencies. Between 5 and 35°C these target strength variations may be spread over a band as wide as 12 dB, which decreases to 6 dB if the water temperature is restricted to between 15 and 25°C, and further decreases to 1.5 – 4 dB for frequencies below 200 kHz.

In comparing fluid-filled and air-filled spheres as sonar targets, firstly it is to be noted that the target strength of the former is substantially higher than the latter. Thus a much larger air-filled sphere is required to achieve the same target strength, thereby increasing deployment complexity.

In a sonar detection trial using spheres as the targets, it is likely that the target strength of the "wrong" temperature, and at a "nearby" frequency will be used. For frequencies below 200 kHz and ambient water temperatures between 15 and 25°C, the target strength of a fluid-filled sphere may be in error by 0.4 – 4 dB. For an air-filled sphere, the error may be 1 – 12 dB.

# 5. References

Bobber, R.J. (1988). *Underwater electroacoustic measurements*, Peninsula Publishing, Los Altos, USA, 333 pp.

Chu, D. and Stanton, T.K. (1998). "Application of pulse compression techniques to broadband acoustic scattering by live individual zooplankton", *Journal of the Acoustical Society of America*, **104** (1), 39-55.

Dawe, R.L. (1997). "Threshold detection modelling explained", *DSTO Aeronautical and Maritime Research Laboratory Technical Report DSTO-TR-0586*, Melbourne, 64 pp.

Gaunaurd, G.C. and Werby, M.F. (1991). "Lamb and creeping waves around submerged spherical shells resonantly excited by sound scattering. II: Further applications", *Journal of the Acoustical Society of America*, **89** (4), 1656-1667.

Hampton, L.D. and McKinney, C.M. (1961). "Experimental study of the scattering of acoustic energy from solid metal spheres in water", *Journal of the Acoustical Society of America*, **33** (5), 664-673.

Hickling, R. (1962). "Analysis of echoes from a solid elastic sphere in water", *Journal of the Acoustical Society of America*, **34** (10), 1582-1592.

Hickling, R. (1964). "Analysis of echoes from a hollow metallic sphere in water", *Journal of the Acoustical Society of America*, **36** (6), 1124-1137.

Horton, J.W. (1959). *Fundamentals of sonar*, 2nd ed., United States Naval Institute, Annapolis, 417 pp.

Kaduchak, G. and Loeffler, C.M. (1998). "Relationship between material parameters and target strength of fluid-filled spherical shells in water: calculations and observations", *IEEE Journal of Oceanic Engineering*, **23** (1), 26-30.

Kessel, R.T. and Hollett, R.D. (2008). "The variability of sonar detection range in port protection: theory, observations and applications", *National Undersea Research Center Technical Report NURC-FR-2008-008*, La Spezia, 47 pp.

Kroszczyński, J. J. (1969). "Pulse compression by means of linear-period modulation", *Proceedings of the IEEE*, **57** (7), 1260-1266.

Medwin, H., and Clay, C.S. (1998). *Fundamentals of acoustic oceanography*, Academic Press, San Diego, 712 pp.

Nelson, D.E. (1976). "An automated solution for the wide band sonar equation", in *IEEE International Conference on Acoustics, Speech, and Signal Processing ICASSP '76*, Institute of Electrical and Electronics Engineers, New York, **1**, 682- 685.

Readhead, M. (1995). "Calculations of the sound scattering from fluid-filled spherical shell sonar targets", *DSTO Aeronautical and Maritime Research Laboratory Research Report DSTO-RR-0020*, Melbourne, 88 pp.

Ross, D. (1976). *Mechanics of underwater noise*, Pergamon Press, New York, 375 pp.

Standards Australia (1997). "Pressure vessels", *Australian Standard AS 1210-1997*, Standards Australia, Sydney, 344 pp.

Trevorrow, M.V. (2005). "High-frequency acoustic scattering and absorption effects with ship wakes", *Defence R&D Canada - Atlantic Scientific Literature DRDC-ATLANTIC-SL-2005-125*, Dartmouth, 8 pp.

Urick, R.J. (1962). "Generalised form of the sonar equations", *Journal of the Acoustical Society of America*, **34** (5), 547-550.

Urick, R.J. (1983). *Principles of underwater sound*, 3rd ed., McGraw-Hill, Los Altos, USA, 423 pp.

Werby, M.F. (1990). "Scattering in the time domain from submerged elastic shells at coincidence frequencies", in *Proceedings of OCEANS '90, 'Engineering in the ocean environment'*, Institute of Electrical and Electronics Engineers, New York, 572-575.

Werby, M.F. and Chin-Bing, S.A. (1991). "Large resonance signatures in scattering from submerged elastic targets in the time and frequency domain", in *Proceedings of OCEANS '91, 'Ocean technologies and opportunities in the Pacific for the 90's'*, Institute of Electrical and Electronics Engineers, New York, **3**, 1352-1360.

Werby, M.F. and Gaunaurd, G.C. (1991). "Critical frequencies for large scale resonance signatures from elastic bodies", *Proceedings of SPIE, 'Automatic object recognition'*, ed. F.A. Sadjadi, **1471**, 2-17.

Werby, M.F. and Gaunaurd, G.C. (1992). "Strong resonance features present in the acoustic signatures of submerged elastic structures", *Optical Engineering*, **31** (12), 2562-2571.

Williams, R.E. and H.F. Battestin (1976). "Time coherence of acoustic signals transmitted over resolved paths in the deep ocean", *Journal of the Acoustical Society of America*, **59** (2), 312-328.

# 6. Errata

Four equations in Appendix C of Readhead (1995) contain typographical errors, in which an exponent 2 is missing. These equations should be:

$$\gamma_{53} = \left(k_T b\right)^2 j_l''\left(k_T b\right) + \left[l\left(l+1\right) - 2\right] j_l\left(k_T b\right) \tag{C25}$$

$$\gamma_{54} = \left(k_T b\right)^2 n_l''\left(k_T b\right) + \left[l\left(l+1\right) - 2\right] n_l\left(k_T b\right) \tag{C26}$$

$$\gamma_{63} = \left(k_T a\right)^2 j_l''\left(k_T a\right) + \left[l\left(l+1\right) - 2\right] j_l\left(k_T a\right) \tag{C29}$$

$$\gamma_{64} = \left(k_T a\right)^2 n_l''\left(k_T a\right) + \left[l\left(l+1\right) - 2\right] n_l\left(k_T a\right) \tag{C30}$$

**DEFENCE SCIENCE AND TECHNOLOGY ORGANISATION**
**DOCUMENT CONTROL DATA**

1. PRIVACY MARKING/CAVEAT (OF DOCUMENT)

2. TITLE

Calculations of the Sound Scattering of Hyperbolic Frequency Modulated Chirped Pulses from Fluid-filled Spherical Shell Sonar Targets

3. SECURITY CLASSIFICATION (FOR UNCLASSIFIED REPORTS THAT ARE LIMITED RELEASE USE (L) NEXT TO DOCUMENT CLASSIFICATION)

| | |
|---|---|
| Document | (U) |
| Title | (U) |
| Abstract | (U) |

4. AUTHOR(S)

Mark Readhead

5. CORPORATE AUTHOR

DSTO Defence Science and Technology Organisation
PO Box 1500
Edinburgh South Australia 5111 Australia

| 6a. DSTO NUMBER | 6b. AR NUMBER | 6c. TYPE OF REPORT | 7. DOCUMENT DATE |
|---|---|---|---|
| DSTO-RR-0351 | AR-014-725 | Research Report | February 2010 |

| 8. FILE NUMBER | 9. TASK NUMBER | 10. TASK SPONSOR | 11. NO. OF PAGES | 12. NO. OF REFERENCES |
|---|---|---|---|---|
| U 490-6-309 | DMO 07/102 | DGMSS | 36 | 24 |

13. URL on the World Wide Web

http://www.dsto.defence.gov.au/corporate/reports/DSTO-RR-0351.pdf

14. RELEASE AUTHORITY

Chief, Maritime Operations Division

15. SECONDARY RELEASE STATEMENT OF THIS DOCUMENT

*Approved for public release*

OVERSEAS ENQUIRIES OUTSIDE STATED LIMITATIONS SHOULD BE REFERRED THROUGH DOCUMENT EXCHANGE, PO BOX 1500, EDINBURGH, SA 5111

16. DELIBERATE ANNOUNCEMENT

No Limitations

17. CITATION IN OTHER DOCUMENTS Yes

18. DSTO RESEARCH LIBRARY THESAURUS http://web-vic.dsto.defence.gov.au/workareas/library/resources/dsto_thesaurus.shtml

Acoustic scattering, Target strength, Sonar, Spherical shells, Sonar targets

19. ABSTRACT

The theory of the sound pressure scattered from a fluid-filled spherical shell immersed in a second fluid is developed for the case of ensonification with hyperbolic frequency modulated chirped pulses. Hyperbolic frequency modulation is also known as 'linear period modulation' and 'logarithmic phase modulation'. The theory is used to calculate the target strength of a stainless steel shell filled with a mixture of Freon-113™ and ethanol, and immersed in sea water. The sensitivity of the target strength to pulse centre frequency, pulse bandwidth, pulse length and fluid temperature is examined and significant sensitivity is found in some cases, especially for temperature. The signal reflected by the target is shown as a function of time, and the results of correlating the return with a replica of the transmitted signal are also shown. Comparison is made with a solid stainless steel sphere and air-filled spherical shells, and similar parameter sensitivity is found, with the exception that their target strengths are insensitive to temperature.